

OVERVIEW OF GEOPHYSICAL SIGNATURES ASSOCIATED WITH CANADIAN ORE DEPOSITS

K. FORD, P. KEATING, AND M.D. THOMAS

*Geological Survey of Canada, 601 Booth Street, Ottawa, Ontario K1A 0E8
Corresponding author's email: KFord@nrcan.gc.ca*

Abstract

Canadian ore deposits have typical geophysical signatures, either at regional or detailed scales. The particular geophysical response of an ore deposit depends on the contrast between its physical properties and those of its host rock. The most important physical properties are density, magnetic susceptibility, electrical conductivity and chargeability, and radioactivity. Density and susceptibility contrasts have a local influence on the measurement of the Earth's gravity and magnetic fields. Electrical properties contrasts can be detected using natural fields, as in magnetotelluric methods, or by artificial electromagnetic fields. Radioactivity is a natural phenomenon and is related to the chemico-physical nature of the rocks and minerals. Some types of deposits do not have any direct geophysical response; the best example is gold mineralization. In that case, geophysics is used in an indirect fashion to map favourable structures that have a good geophysical response. Other types of deposits are directly detectable by geophysical techniques. For example, massive sulphide deposits generally produce significant electromagnetic, gravimetric, and magnetic responses.

Here, we first present the principal geophysical techniques currently in use in Canada. Only a brief and simplified description of each method is given since extensive descriptions are available in the geophysical literature. Some typical survey specifications are provided. This is followed by a description of the geophysical responses of the major mineral deposit types found in Canada. In each case, we discuss the physical properties that can give rise to a geophysical response and we present typical examples. Applicability and effectiveness of the techniques are also discussed.

Geophysics was instrumental in the discovery of many Canadian ore deposits. Although there are likely many shallow ore deposits still to be discovered, the next major discoveries are expected to be at greater depth. Hopefully, some current geophysical techniques can detect deposits at depths in excess of one kilometre.

Résumé

Les gîtes minéraux du Canada présentent des signatures géophysiques caractéristiques, que ce soit à l'échelle régionale ou locale. La réponse géophysique particulière d'un gîte dépend du contraste entre ses propriétés physiques et celles des roches encaissantes. Les plus importantes de ces propriétés sont la densité, la susceptibilité magnétique, la conductivité électrique et la chargeabilité ainsi que la radioactivité. Les contrastes de densité et de susceptibilité ont localement une influence sur les champs gravitationnel et magnétique de la Terre. Les contrastes des propriétés électriques peuvent être détectés en ayant recours aux champs naturels, comme le font les méthodes magnétotelluriques, à des champs électromagnétiques artificiels. La radioactivité est un phénomène naturel et est reliée à la nature physico-chimique des roches et des minéraux. Certains types de gîtes ne présentent pas une réponse géophysique directe; le meilleur exemple est celui des minéralisations aurifères. Dans le cas de ces gîtes, la géophysique est appliquée de manière indirecte en permettant la cartographie de structures favorables qui présentent une bonne réponse géophysique. D'autres types de gîtes sont directement détectables par des méthodes géophysiques. Par exemple, les gîtes de sulfures massifs fournissent généralement d'importantes réponses électromagnétiques, gravimétriques et magnétiques.

Nous présentons ici les principales méthodes géophysiques actuellement utilisées au Canada. On ne fournit pour chaque méthode qu'une description brève et simplifiée puisque des descriptions élaborées sont disponibles dans la littérature géophysique. Des spécifications caractéristiques propres à certains types de levés sont offertes, suivies d'une description des réponses géophysiques des principaux types de gîtes au Canada. Dans chaque cas, nous discutons les propriétés physiques qui engendrent la réponse géophysique et présentons des exemples caractéristiques. L'applicabilité et l'efficacité des méthodes sont en outre discutées.

La géophysique a contribué à la découverte d'un grand nombre de gîtes minéraux du Canada. Bien qu'il reste vraisemblablement un grand nombre de gisements peu profonds à découvrir, les prochaines découvertes majeures se feront probablement à plus grande profondeur. Certaines des méthodes géophysiques courantes permettent heureusement la détection de gisements à des profondeurs excédant un kilomètre.

Introduction

This paper is a contribution to the Consolidating Canada's Geoscience Knowledge program, providing a synthesis of geophysical signatures that are associated with the nine major mineral deposit types addressed in this program. The detection of mineral deposits by geophysical methods is dependent primarily on a single factor, namely that the deposit displays physical or chemical attributes that differ significantly from those of the adjacent rock formations. Historically, the principal physical properties that have been the focus of geophysical exploration methods are density, magnetization (induced and remanent), conductivity, chargeability, radioactivity, and seismic velocity. The latter has

generally been associated with the petroleum industry, though in recent years it has found increasing application in the search for orebodies.

Sometimes the desired deposit-type or mineralized target has a physical property (or properties) that permits direct discovery, for example Pb-Zn deposits (galena-sphalerite) have high densities that may be detected directly by a gravity survey. On the other hand, many base metal deposits are discovered by virtue of the physical properties of an associated non-economic mineral. A good example is a Cu-rich (chalcopyrite) volcanic massive sulphide (VMS) deposit targeted on the basis of a strong magnetic anomaly produced by genetically related pyrrhotite. Technically, this should be

considered as indirect detection. However, because of the close spatial and genetic relationship between the pyrrhotitic orebody and the desired commodity (chalcopyrite), we consider this as a direct discovery, and would include in the same category the discovery of diamonds, which have a spatial and genetic association with their kimberlitic hosts. Again, signatures of physical and/or chemical properties of alteration assemblages associated with mineralizing processes, which may extend well beyond the economically mineralized target (e.g. K alteration), and which in principle could be categorized as an indirect target, are also classified as direct targets for the purpose of this report.

Geophysical surveys also often provide critical information in support of local or regional framework mapping and mineral exploration modeling, and this aspect is termed framework mapping.

In this report, a brief discussion of physical and chemical properties of ore, ore-associated minerals, and their hosts is presented, together with summary descriptions of the more commonly used geophysical methods that are based on these properties. The geophysical methods and their characteristic signatures are also illustrated in the context of several mineral deposit types.

Borehole geophysical logging is another aspect of geophysical exploration that employs a suite of methodologies to measure the aforementioned physical properties or related characteristics, and also commonly measures temperature. This subject is not discussed in this presentation.

Physical and Chemical Properties of Ore Minerals, Ore-Related Minerals and Common Lithologies

It has been noted that contrasts between the physical properties of ore minerals, together with ore-related minerals, and host rocks are critical to the successful application of geophysical methods. Chemical properties are included to cover properties measured by gamma-ray spectrometry surveys, which estimate abundances of K, Th, and U. Densities, magnetic susceptibilities, and electrical conductivities for several ore minerals, ore-associated minerals, and common rock types that may host mineral deposits are presented in Table 1. A complementary list of radioelement concentrations for several classes of rocks is provided in Table 2.

Principal Geophysical Exploration Methods

Geophysical methods have been applied in the search and delineation of orebodies in Canada since at least the beginning of the 20th century. Belland (1992), for example, reported use of a dip-needle magnetometer to map the Austin Brook iron deposit in the Bathurst Mining Camp, New Brunswick in 1903/04. Most of the first half of the 20th century witnessed the development and application of the magnetic, gravity, electrical, seismic, and radiation methods, all applied on the ground. Then, in the late 1940s, following World War II, magnetic and electromagnetic methods became airborne as a consequence of new technology developed during the war. Since that time, geophysical exploration has evolved tremendously in terms of instrumentation, acquisition, processing, global positioning, and analysis, benefiting from the parallel evolution of electronic computers. Examples of modern fixed-wing and rotary-wing aircraft

TABLE 1. Physical properties (density, magnetic susceptibility, electrical conductivity) of some common rock types, ore minerals, and ore-related minerals (from Thomas et al., 2000).

Rock Type	Density g/cm ³			Magnetic SI x 10 ⁻³			Conductivity mS/m		
	Min.	Max.	Ave.	Min.	Max.	Ave.	Min.	Max.	Ave.
Sediments and Sedimentary Rocks									
Overburden				1.92					
Soil	1.2	2.4	1.92	0.01	1.26				
Clay	1.63	2.6	2.21				10	300	
Glaciolacustrine Clay						0.25	10	200	
Gravel	1.7	2.4	2				0.1	2	
Sand	1.7	2.3	2				0.1	2	
Glacial Till							0.5	20	
Saprolite (mafic volcanic rocks, schist)							50	500	
Saprolite (felsic volcanic rocks, granite, gneiss)							5	50	
Sandstone	1.61	2.76	2.35	0	20	0.4	1	20	
Shale	1.77	3.2	2.4	0.01	18	0.6	30	200	
Argillite							0.07	83.3	
Iron Formation							0.05	3300	
Limestone	1.93	2.9	2.55	0	3	0.3	0.01	1	
Dolomite	2.28	2.9	2.7	0	0.9	0.1	0.01	1	
Conglomerate							0.1	1	
Greywacke	2.6	2.7	2.65				0.09	0.24	
Coal			1.35				0.03	2	100
Red Sediments			2.24	0.01	0.1				
Igneous Rocks									
Rhyolite	2.35	2.7	2.52	0.2	35				0.04
Andesite	2.4	2.8	2.61				160		
Granite	2.5	2.81	2.64	0	50	2.5			
Granodiorite	2.67	2.79	2.73						
Porphyry	2.6	2.89	2.74	0.3	200	60			
Quartz Porphyry				0	33	20	0.04	1.7	
Quartz Diorite	2.62	2.96	2.79						
Quartz Diorite, Dacite				38	191	83			
Diorite	2.72	2.99	2.85	0.6	120	85			
Diabase	2.5	3.2	2.91	1	160	55			0.03
Olivine Diabase							25		
Basalt	2.7	3.3	2.99	0.2	175	70			0.2
Gabbro	2.7	3.5	3.03	1	90	70			0.02
Hornblende Gabbro	2.98	3.18	3.08						
Peridotite	2.78	3.37	3.15	90	200	250			
Obsidian	2.2	2.4	2.3						
Pyroxenite	2.93	3.34	3.17				125		
Monzonite, Latite				33	135	85			
Acid Igneous Rocks	2.3	3.11	2.61	0	80	8			
Basic Igneous Rocks	2.09	3.17	2.79	0.5	97	25			
Mafic Volcanic Rocks							0.09	0.27	
Dacite	2.35	2.8	2.58						
Phonolite	2.45	2.71	2.59						
Trachyte	2.42	2.8	2.6	0	111	49			
Nepheline Syenite	2.53	2.7	2.61						
Syenite	2.6	2.95	2.77	0	111	49			
Anorthosite	2.64	2.94	2.78						
Norite	2.7	3.24	2.92						
Metamorphic Rocks									
Quartzite	2.5	2.7	2.6				4		
Schist	2.39	2.9	2.64	0.3	3	1.4			
Marble	2.6	2.9	2.75						
Serpentine	2.4	3.1	2.78	3	17				
Slate	2.7	2.9	2.79	0	35	6			
Gneiss	2.59	3	2.8	0.1	25				
Amphibolite	2.9	3.04	2.96				0.7		
Eclogite	3.2	3.54	3.37						
Granulite	2.52	2.73	2.65	3	30				
Phyllite	2.68	2.8	2.74				1.5		
Quartz Slate	2.63	2.91	2.77						
Chlorite Schist	2.75	2.98	2.87						
Skarn	2.95	3.15				2.5			1.25
Hornfels	2.9	3				0.31			0.05
Sulphide Minerals									
Chalcopyrite	4.1	4.3	4.2	0.02	0.4		1.11	6.67	
Galena	7.4	7.6	7.5			-0.03	1.11	1.47	
Pyrite	4.9	5.2	5	0.03	5.3		1.67	8.33	
Pyrrhotite	4.9	5.2	5		3200		6.25	5.00	
Sphalerite	3.5	4	3.75	-0.03	0.75		0.08	3.70	
Other									
Magnetite				5.04	1000	5700			1.92
Graphite	1.9	2.3	2.5	-0.08	0.2		1.01	3.57	

Compiled from Grant and West (1965), Keller and Frischknecht (1966), Carmichael (1982)
Hunt et al. (1995), Palacky (1986), and Telford et al. (1990).

Overview of Geophysical Signatures Associated with Canadian Ore Deposits

fitted with magnetometer, electro-magnetic, and gamma-ray spectrometer installations are illustrated in Figure 1.

Magnetic Method

The magnetic method is the oldest and most widely used geophysical exploration tool. An early discovery of a Canadian ore deposit by an aeromagnetic survey was that of the Marmora iron ore deposit in Ontario in 1949 (Reford, 1980). The effectiveness of the method depends mainly on the presence of magnetite in the rocks of the surveyed area. Another important magnetic mineral is pyrrhotite. The primary goal of magnetic surveys is direct detection of metallic ore-bodies through delineation of associated anomalies. Another objective is to determine trends, extents, and geometries of magnetic bodies in an area, and to interpret them in terms of geology. The technique is particularly effective in areas

TABLE 2. Radioelement concentrations in different classes of rocks (after Killeen, 1979).

Rock Type	Potassium (%)		Uranium (ppm)		Thorium (ppm)	
	Mean	Range	Mean	Range	Mean	Range
Acid Extrusives	3.1	1.0-6.2	4.1	0.8-16.4	11.9	1.1-41.0
Acid Intrusives	3.4	0.1-7.6	4.5	0.1-30.0	25.7	0.1-253.1
Intermediate Extrusives	1.1	1.1-2.5	1.1	0.2-2.6	2.4	0.4-6.4
Intermediate Intrusives	2.1	0.1-6.2	3.2	0.1-23.4	12.2	0.4-106.0
Basic Extrusives	0.7	0.06-2.4	0.8	0.03-3.3	2.2	0.05-8.8
Basic Intrusives	0.8	0.01-2.6	0.8	0.01-5.7	2.3	0.03-15.0
Ultrabasic	0.3	0-0.8	0.3	0-1.6	1.4	0-7.5
Alkali Feldspathoidal Intermediate Extrusives	6.5	2.0-9.0	29.7	1.9-62.0	133.9	9.5-265.0
Alkali Feldspathoidal Intermediate Intrusives	4.2	1.0-9.9	55.8	0.3-720.0	132.6	0.4-880.0
Alkali Feldspathoidal Basic Extrusives	1.9	0.2-6.9	2.4	0.5-12.0	8.2	2.1-60.0
Alkali Feldspathoidal Basic Intrusives	1.8	0.3-4.8	2.3	0.4-5.4	8.4	2.8-19.6
Chemical Sedimentary Rocks	0.6	0.02-8.4	3.6	0.03-26.7	14.9	0.03-132.0
Carbonates	0.3	0.01-3.5	2	0.03-18.0	1.3	0.03-10.8
Detrital Sedimentary Rocks	1.5	0.01-9.7	4.8	0.01-80.0	12.4	0.2-362.0
Metamorphosed Igneous Rocks	2.5	0.1-6.1	4	0.1-148.5	14.8	0.1-104.2
Metamorphosed Sedimentary Rocks	2.1	0.01-5.3	3	0.1-53.4	12	0.1-91.4

where few outcrops exist. Structural trends are faithfully reproduced in magnetic patterns, but assignment of rock type is ambiguous, since ranges of values of magnetic susceptibilities of different rock types may overlap (Table 1).



FIGURE 1. (A) Cessna 208B Caravan aircraft fitted with a magnetometer in the rear stinger. Image source: Sander Geophysics web site (www.sgl.com/pic_air.htm); (B) de Havilland Dash 7 aircraft fitted with a MEGATEM electromagnetic system (Fugro Airborne Surveys). Photo courtesy of Régis Dumont, Geological Survey of Canada; (C) Large volume (50.4 litres) airborne gamma ray spectrometer installation in a Cessna 208B Caravan aircraft. Photo courtesy of R.B.K. Shives, Geological Survey of Canada; (D) Eurocopter Astar 350B3 helicopter with a magnetometer in the forward mounted stinger and a gamma ray spectrometer system consisting of 33 litres of NaI detectors.

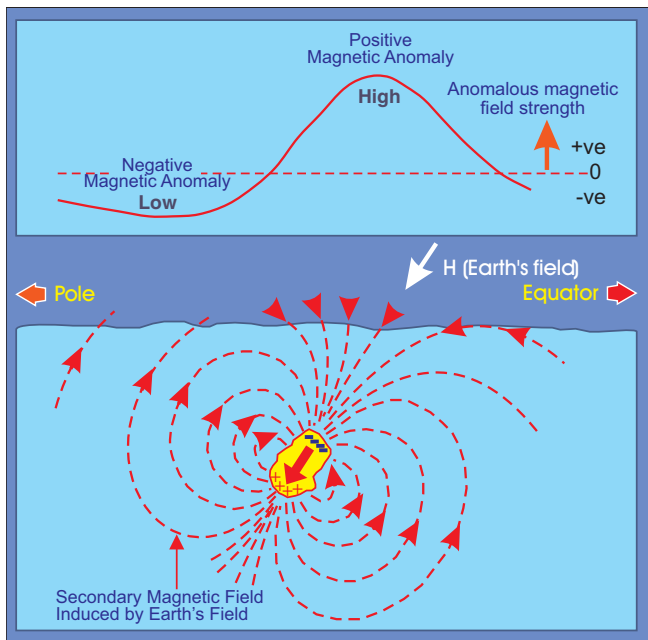


FIGURE 2. Induced magnetization in a geological body produces a local positive magnetic anomaly and a subsidiary negative anomaly.

Susceptibility may vary considerably, even within the same rock type.

In magnetic surveys, the intensity or strength of the Earth's total magnetic field is measured. The intensity of the total magnetic field over Canada ranges from about 52000 to more than 60000 nT. The total field includes contributions from the Earth's core and crust. A third component, originating from electrical currents in the upper atmosphere, is normally eliminated from survey data during processing. It is common practice to subtract the component of the field attributed to the Earth's core, described mathematically by the International Geomagnetic Reference Field, from the total field. The resultant field is termed the residual total magnetic field, and depending on location, values may be positive or negative. The Earth's magnetic field induces a secondary magnetic field in magnetic geological bodies, which locally enhances the Earth's field producing local positive culminations or anomalies (Fig. 2). Because of the dipolar nature of magnetization, negative anomalies may also be generated, though at high magnetic latitudes, such as within Canada, they are generally of low amplitude. The presence of reversed remanent magnetizations can, however, produce prominent negative anomalies.

Several derivatives of the residual total magnetic field provide value-added products that may contribute to the geological interpretation of magnetic data. They include maps of the first vertical derivative (= vertical gradient), 2nd vertical derivative, analytic signal, and tilt. The first vertical derivative (nT/m) is probably the most commonly used derived product. It may be derived mathematically from the total magnetic field, or alternatively it may be measured directly using a gradiometer, comprising two magnetometers separated vertically by 2 to 3 metres. Vertical gradient maps present a filtered picture of the magnetic field, emphasizing near-surface geological features. Gradient anomalies are narrower than corresponding total field features, hence magnetic

anomalies produced by closely spaced geological units are better resolved by the vertical gradient. Vertical gradient maps are useful for mapping geological contacts, since theoretically the zero contour of the gradient coincides with contacts between contrasting magnetizations, provided the contacts are steep and the area is in high magnetic latitudes (Hood and Teskey, 1989).

Electrical Methods

Electrical methods, in common with the electromagnetic techniques, respond to the electrical conductivity of rocks and minerals, which may vary by 20 orders of magnitude (Grant and West, 1965). No other physical property varies that much. Native metals, such as copper and silver, are highly conductive, whereas minerals such as quartz are, for all practical purposes, nonconductive. Rock and mineral conductivity is a complex phenomenon. Current can be propagated in three different ways by electronic (= ohmic), electrolytic or dielectric conduction. Electronic conduction is effected by the presence of free electrons, and is the means by which current flows in metals. In electrolytic conduction, the current is carried by ions, and flows at a slower rate. In dielectric conduction, the current is known as the displacement current. In this case, there are very few or no current carriers and the electrons are slightly displaced relative to the atomic nuclei by an externally varying electric field. This very small separation between negative and positive charges is known as the dielectric polarization and produces the displacement current.

The electrical conductivity of rocks and mineral deposits is commonly measured in milliSiemens per metre (mS/m). Granite is essentially non-conductive, whereas the conductivity of shale ranges from 0.5 to 100 mS/m. Water content increases conductivity and may have a dramatic influence on its magnitude. Wet and dry tuffs, for example, have conductivities that differ by a factor of 100 (Telford et al., 1990). Different rock types have overlapping ranges of conductivity. The conductivities of massive sulphides may overlap those of other, nonmineralized materials such as graphite and clays. Conductive overburden, especially water-saturated clays, may generate electromagnetic anomalies that effectively mask the response of an underlying massive sulphide zone. Unequivocal identification of mineral deposits is, therefore, a difficult task. Where the conductivity of overburden is sufficiently uniform, the electromagnetic responses can be interpreted in terms of overburden thickness. Conductivity and resistivity are the inverse of each other, and both terms are commonly used.

Conductivities of common rocks and minerals are listed in Table 1. Massive sulphides, graphite, and salt water have high conductivities, exceeding 500 mS/m. Intermediate values, between 1 and 500 mS/m, are typical of sedimentary rocks, glacial sediments, weathered rock, alteration zones, and fresh water. Igneous and metamorphic rocks have low conductivities, less than 1 mS/m.

A number of electrical (and electromagnetic) techniques have been developed to take advantage of the high variability of rock and mineral conductivities. Electrical methods are applied on the ground, whereas electromagnetic methods may be employed on the ground or in the air using different

airborne platforms. Some, like self-potential and the magnetotelluric method, use natural fields, while others such as DC resistivity or electromagnetic techniques use artificial sources. Here, discussion is restricted to the principal techniques used for mineral exploration.

Electrical Resistivity Surveys

Measurements of resistivity, or rather apparent resistivity, represent one of the oldest geophysical survey techniques. Resistivity surveys are achieved by injecting current into the ground using two electrodes, and measuring the voltage at two other electrodes. Various electrode configurations may be used, but in all cases it is possible to compute the apparent resistivity

of the subsurface at various depths, and the data can be used to generate a cross-section of the true resistivity (Fig. 3). The method is used both for the direct detection of orebodies, such as Mississippi Valley-type sulphide bodies for example, and to define the 3-D geometry of a target, such as a kimberlite pipe. Resistivity surveys are also used to map overburden thickness to help improve interpretation of ground gravity surveys. Conductivity, the inverse of resistivity, is commonly estimated from airborne electromagnetic data and used to map overburden.

Induced Polarization Surveys

Induced polarization (IP) has been used in mineral exploration since the mid-1950s. It is a rather complex phenomenon, but easy to measure. IP measures the chargeability of the ground, i.e. how well materials tend to retain electrical charges. Measurements are made either in the time-domain or the frequency-domain; their units are respectively milliseconds (msec) and percentage frequency effect (PFE). When a voltage applied between two electrodes is abruptly interrupted, the electrodes used to monitor the voltage do not register an instantaneous drop to zero, but rather record a fast initial decay followed by a slower decay. If the current is switched on again, the voltage will first increase at a very high rate and then build up slowly. This phenomenon is known as induced polarization. The technique is mostly concerned with measuring the electrical surface polarization of metallic minerals. This effect is induced by abrupt changes in electrical currents applied to the ground. Disseminated sulphides produce very good induced polarization responses. In theory, massive sulphides should have lower responses, but in practice they have very good responses. This is due to the mineralization halo generally surrounding massive sulphides. Clay minerals may also produce significant IP responses. More details can be found in various textbooks (e.g. Telford et al., 1990).

Induced polarization surveys are carried out along equally spaced lines perpendicular to the main geological strike. Two current electrodes are used to inject current into the ground,

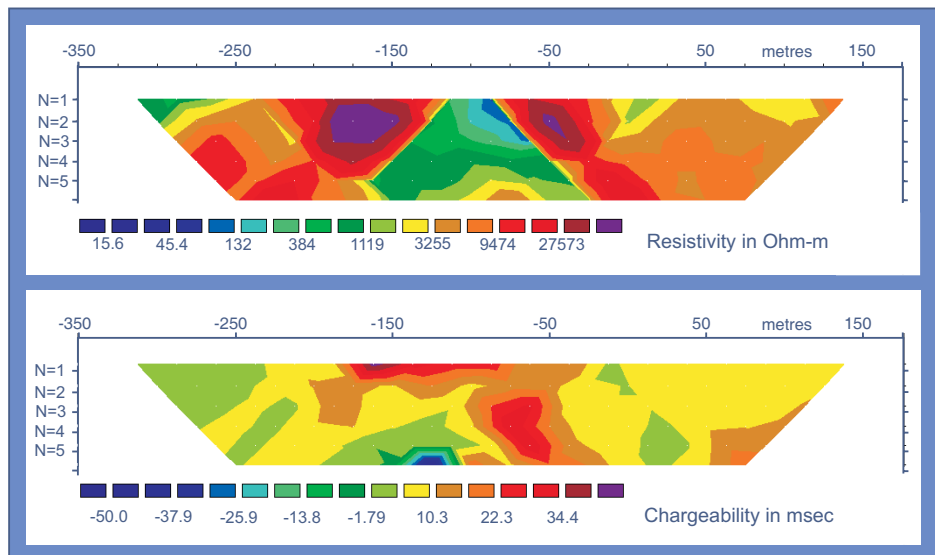


FIGURE 3. Pseudosections of resistivity and chargeability derived from a dipole-dipole resistivity-induced polarization survey. Electrode spacing varies from 1 to 5 m.

and two voltage electrodes are used to measure the decay voltage. Resistivity measurements are made concurrently. Various electrode layouts can be used (pole-dipole, dipole-dipole, etc.); varying the distance between the electrodes results in soundings to different depths, which may be used to map the variability of resistivity and chargeability with depth (Fig. 3). For dipole-dipole surveys, the distance between pairs of electrodes is kept constant and the separation between the voltage and current electrodes is increased. This distance is increased by integer multiples “n” of the distance between the voltage electrodes.

A new system, called Titan-24 developed by Quantec Geoscience, combines IP, resistivity, and magnetotelluric techniques, the latter using the Earth’s natural field. This system can detect conductive deposits at a depth of 1.5 km.

Electromagnetic Methods

Electromagnetic (EM) techniques, both airborne and ground, are among the most commonly used methods in mineral exploration. They are capable of direct detection of conductive base-metal deposits, where large conductivity contrasts exist between the deposits and resistive host-rocks or thin overburden cover. The techniques have been highly successful in North America and Scandinavia. A multitude of other conductive sources, including swamps, shear and fracture zones, faults, and graphitic and barren metallic conductors, create a major source of ambiguity in the interpretation of EM anomalies.

Electromagnetic systems operate in either the frequency or the time domain. In either method, an EM field is transmitted, which on penetrating the ground and encountering conductive material generates a secondary field that may be measured by a receiver. The concept is illustrated for an airborne time-domain system in Figure 4. Different combinations and geometries of transmitters and receivers may be used.

In frequency-domain systems, a transmitter creates an alternating EM field. This primary field generates eddy cur-

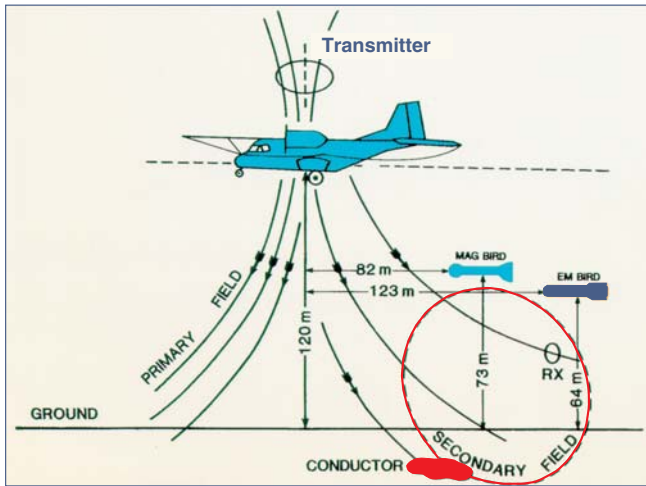


FIGURE 4. Schematic of one type of airborne electromagnetic system – in this case, a time-domain system (modified after Rowe et al., 1995).

rents in a conductive medium, which in turn produces a secondary EM field. This secondary field, detected by the receiver, is diagnostic of the electrical characteristics of the conductive medium excited by the primary field. In general, the secondary field is not in phase with the primary field. The EM receiver measures the in-phase and out-of-phase (quadrature) components of the secondary field, and the ratio of the secondary field to the primary field in parts per million (ppm). Time-domain electromagnetic systems transmit very short pulses. In general, these pulses last for a few milliseconds and are a few milliseconds away from each other. Pulses can have various shapes: half-sine, step, ramp, etc. For example, the MEGATEM airborne time-domain EM system often operates with a base frequency of 90 Hz, it uses half-sine pulses of 2 milliseconds, and pulses of opposite polarity are transmitted every 5.5 milliseconds. All such systems have a broad frequency range. The secondary field time-decay curve begins immediately at the end of the transmitter cut-off.

As EM responses are frequency dependent, modern airborne electromagnetic (AEM) systems use a wide range of frequencies to detect a large range of conductivities. A number of configurations for the transmitter and receiver coils are used to discriminate between horizontal and vertical conductors. The coplanar coil pair is more sensitive to horizontal conductors, while the coaxial coil pair is more sensitive to vertical conductors. The geometry and attitude (dip) of conductors also influence the shape of the anomalies. For a symmetric EM system, a vertical conductor produces a double peak anomaly when detected by the coplanar coil pair, and a single peak anomaly when measured by the coaxial coil pair (Fig. 5). It should be noted that fixed-wing time-domain electromagnetic systems are asymmetric because the receiver is towed behind and below the transmitter; this results in asymmetric responses that can also be interpreted in terms of dips (Fig. 6).

In the case of frequency-domain EM systems, a geologic formation that has high magnetic susceptibility and low conductivity will generate a large magnetic anomaly and a strong negative in-phase EM response that is opposite to the polarity of the response of a conductive body. In this situa-

tion, the AEM response is likely to reflect a shallower portion of the causative body than the magnetic response. It is also possible to determine the magnetic susceptibility of a rock and evaluate its magnetite content from AEM data (Fraser, 1973).

Airborne EM data can be converted into ground conductivities to produce a conductivity map. To obtain stable results, a number of simplifying assumptions or models must be employed. A homogeneous half-space model (Seigel and Pitcher, 1978), a model bounded by one plane surface (the upper part is infinitely resistive, e.g. air, while the bottom part has a finite resistivity and represents the Earth), assumes that the conductivity of the ground is uniform and that the Earth is flat and bottomless. This model is robust and generally provides realistic results. A second model is based on a single-layer earth, in which a homogeneous conductive layer of uniform thickness overlies a homogeneous half-space.

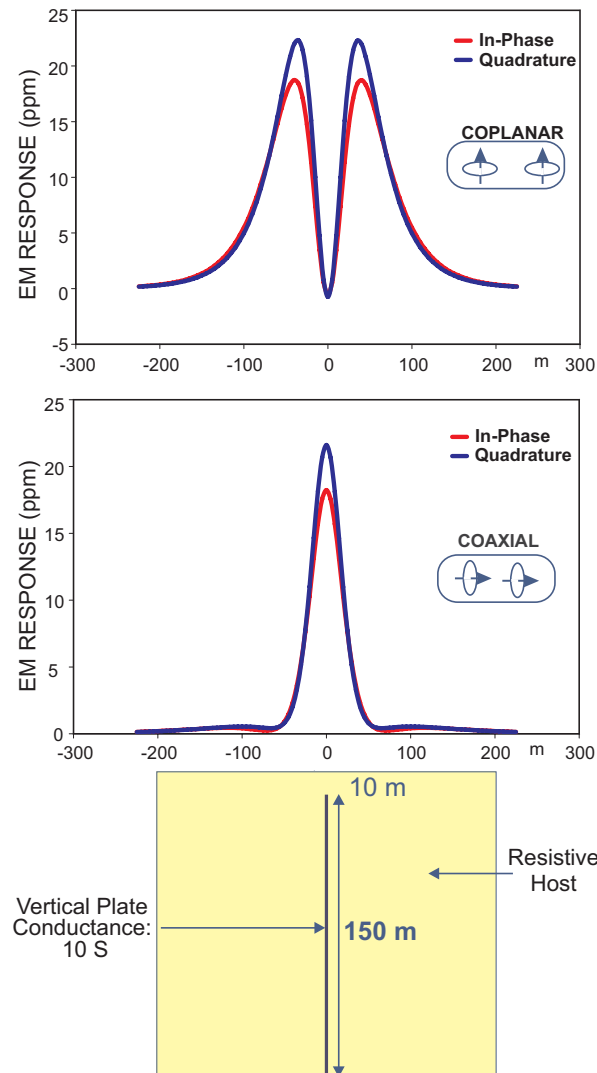


FIGURE 5. Electromagnetic in-phase and quadrature responses for a conductive thin vertical plate (conductance = 10 S; strike length = 300 m) hosted by a resistive (unresponsive) medium. Computation of the profiles assumes a transmitter frequency of 914 Hz and a survey elevation of 30 m above ground surface; the top of the plate is 10 m below surface. Transmitter-receiver coil separation is 7 m.

However, when the top layer is conductive and relatively thin, only the conductivity-thickness product can be determined. Conductance may be determined using a vertical half-plane model (Ghosh, 1972) in free space.

Apparent conductivity may be calculated for any measured frequency, different frequencies providing conductivity information for different parts of the crustal column. For example, in the Bathurst Mining Camp, conductivities calculated from mid-frequency (4433 Hz) coplanar EM data using a homogeneous half-space model best reflect the bedrock geology of the area. Conductivities calculated from low-frequency data (853 and 914 Hz) are generally associated with lithologies having high conductivity contrasts, whereas conductivities calculated from the high frequency EM data (32290 Hz) usually contain significant overburden responses.

The maximum depth at which a deposit can be detected by EM techniques depends on the size of the deposit, its conductivity, and the conductivity of the host rock and the overburden. Typically airborne time-domain EM can detect deposits/conductors at a depth of 250 m in the Abitibi mining belt, and as deep as 750 m in the Athabasca Basin. Ground time-domain EM techniques using large loops can detect conductive targets at depths in excess of 1 km.

Gamma-Ray Spectrometric Method

Early instruments measured only the total radioactivity from all sources, and were used primarily for uranium exploration. The first portable Geiger-Muller counters were built in 1932 at the University of British Columbia by G.M. Shrum and R. Smith and were tested on Quadra Island off the coast of British Columbia (Lang, 1953). The first practical portable counters were developed in the 1940s at the National Research Council (NRC) and used in 1944 by joint Geological Survey of Canada and NRC field crews on Great Bear Lake (Lang, 1953). The first scintillation counters were developed in 1949 and first used in ground radiation surveys of pitchblende deposits in the Lake Athabasca region (Brownell, 1950). In the 1960s, gamma-ray scintillation spectrometers were developed and calibrated to measure discrete windows within the spectrum of gamma-ray energies. This permitted determination of concentrations of individual radioelements.

Potassium (K), uranium (U), and thorium (Th) are the three most abundant, naturally occurring radioactive elements (Table 2). Their abundances (Table 2) and chemical properties provide insight into ore-related processes. For example, K is a major constituent of most rocks and is diagnostic of alteration associated with many mineral deposits; U and Th, usually present in trace amounts, are relatively mobile and immobile elements, respectively, under most surface conditions and are effective in the direct detection of mineralized rocks. Given the various physical and chemical characteristics of the radioactive daughter products in the ^{238}U decay series, disequilibrium can be a significant source of error. Disequilibrium occurs when one or more of the daughter products in the decay series is removed or added. In areas with extreme surficial weathering, disequilibrium is a significant concern. In Canada, due to recent glaciation, disequilibrium due to weathering is less of a concern.

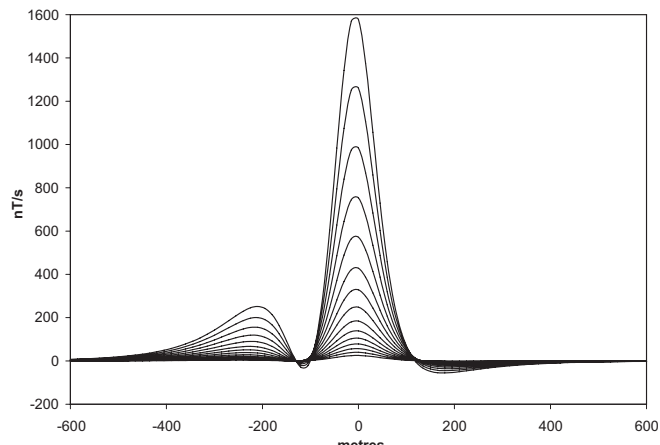


FIGURE 6. Response of the x-component (along line) of an airborne electromagnetic time-domain system (Megateam II). The conductor is a thin vertical plate having a conductance of 20 S, located at $x = 0$ and 120 m under the transmitter. The plane is flying from left to right. Note the presence of 2 peaks. The leading peak is an effect of the asymmetry of the system. The receiver is located in a bird 50 m under the transmitter and 130 m behind it.

Concentrations of uranium and thorium, when measured by gamma-ray spectrometry, are often reported as “equivalent uranium” (eU) and “equivalent thorium” (eTh) as a reminder that the measurement is based on the assumption that equilibrium exists. However, the Th decay series is almost always in equilibrium.

The effectiveness of gamma-ray spectrometry in geological mapping and mineral exploration depends on several factors: the extent to which measurable differences in the radioactive-element distributions relate to bedrock differences (normal lithological signatures); the extent to which these normal signatures are modified by mineralizing processes (K alteration); the extent to which the ore or associated alteration signatures are incorporated into surficial materials; and whether these surficial materials can be spatially related to bedrock sources. A schematic illustration of gamma-ray spectrometry anomalies associated with a porphyry Cu deposit is presented in Figure 7.

The attenuation of gamma rays by rock or soil prevents their emanation from depths greater than approximately 60 cm. This has profound implications for the interpretation of gamma-ray spectrometry surveys. Whereas magnetic, electromagnetic, gravimetric, or seismic sensors may detect features to depths of tens or hundreds of metres, often buried far below the mappable near-surface geology, gamma-ray data are interpretable in terms of the near-surface chemical composition of rocks and soils. A poor correlation between K, eU, and eTh distributions and other layers, such as magnetic or geological layers, reflects the inherently different sampling methods, and greater depth of penetration of the latter. In airborne surveys, a single measurement provides an estimate of the average surface concentration for an area of several thousand square metres. This single sample comprises variable proportions of exposed bedrock (fresh or weathered), overburden (wide variety possible – glacial tills, glacio-fluvial, colluvium, alluvium, loess), soils (clay, sand, loam, etc.) soil moisture, standing water (lakes, rivers, swamps, bogs), and vegetation. In almost all cases, the inhomogeneous nature of the surface (and therefore of each sam-

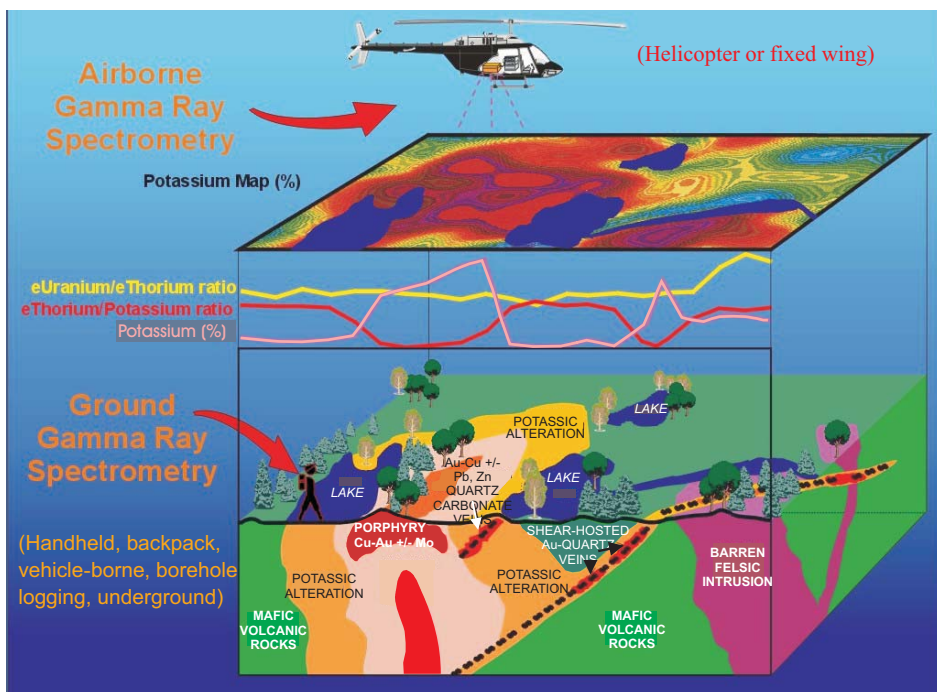


FIGURE 7. Schematic image of airborne and ground gamma-ray spectrometry anomalies associated with a porphyry Cu deposit. Figure courtesy of R.B.K Shives, Geological Survey of Canada.

ple) introduces variability such that the absolute value of K, eU, or eTh may be far less significant than the radioelement patterns. While K, eU, and eTh concentrations are considered to be the primary measured variables of a gamma-ray spectrometry survey, several derived products can provide important value-added information. These include total radioactivity (measured or derived), radioactive element ratios (eU/eTh, eU/K, and eTh/K), and the ternary radioelement map (Broome et al., 1987).

The effects of variations in soil moisture, amount of bedrock exposure, or source geometry can be minimized through the use of radioelement ratios. In mineralized systems, all three radioelements may be enriched or depleted relative to unaltered host rocks. However, one or more of the radioelements may be preferentially affected for valid geochemical reasons. In these cases, the ratios offer very sensitive alteration vectors, which may lead directly or indirectly to the mineralization, even where the individual radioelement patterns are ambiguous.

Gamma-ray spectrometry is particularly effective in granite- and gneiss-dominated terrains where radioactive element concentrations and contrasts are usually the highest (Table 2). However, depending on the flight-line spacing and radioactive element contrasts between different rock types, the technique may be effective in a variety of terrains. When airborne surveys employ both a magnetometer and gamma-ray spectrometer, the two techniques are often complementary, particularly in areas of complex geology.

Gravity Method

Gravity observations provide a measure of the Earth's gravity field, which is sensitive to variations in rock density. Local mass excesses or deficiencies produce, respectively, increases or decreases in the gravity field. These departures from the immediate background level are termed positive

(Fig. 8) and negative anomalies, respectively. The unit of measurement used in geophysical studies is the milligal (mGal). In exploration for base metals, the gravity technique is commonly applied in follow-up investigations of magnetic, electrical, electromagnetic, or geochemical anomalies, and is particularly useful in assessing whether a conductivity anomaly is related to low-density graphite or a higher density sulphide deposit. It is also used as a primary exploration tool to detect the excess masses of base metal sulphide deposits. Gravity data may be used to estimate the size and tonnage of orebodies, and also contribute to exploration programs when used to map geology and structure that may favour the presence of ore deposits. Traditionally, gravity surveys have been carried out on the ground or on ice during winter. Surveys on water bodies have been accomplished

on board ships, typically using specially designed marine gravity meters, and in some cases remotely controlled land gravity meters adapted for deployment on the ocean floor or a lake bottom (e.g. Goodacre et al., 1969). In recent years, significant improvements in the acquisition of airborne gravity data have made airborne surveys more attractive, in spite of the lower accuracy and resolution of the data. On the plus side, airborne surveys provide rapid coverage of large areas along flight-lines spaced much closer together than the spacing between available ground gravity observations that have been made as part of Canada's national gravity mapping program. Airborne surveys, therefore, provide a viable tool for upgrading gravity coverage in

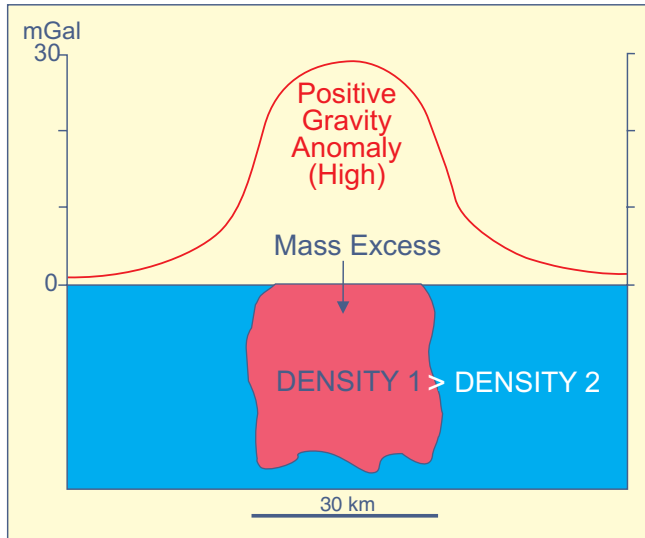


FIGURE 8. An excess mass in the crust locally enhances the gravity field producing a positive anomaly or gravity high.

most parts of Canada, and for establishing regional to semi-regional geological frameworks.

More promising for the direct detection of orebodies is airborne “tensor gravity”. The method measures the gravity tensor, which includes nine tensor components corresponding to gravity gradients along three orthogonal directions, using a highly sensitive gravity gradiometer. One of the components of the tensor is the vertical gravity gradient. The tensor method has high resolution and can detect small targets, such as kimberlites, which characteristically have diameters of only a few hundred metres. At the present time, the method is expensive and the number of contractors capable of offering this service is limited. Lane (2004) presents a review and descriptions of the current state of the art of airborne systems.

Besides variations in crustal density, the gravity field is influenced by latitudinal position and changes in elevation. Therefore, several corrections are applied to observed gravity data to isolate variations related to crustal causes. A small correction is made to eliminate the effect of Earth tides. Two corrections are made to negate the elevation factor: the free-air correction (compensates for variation in the distance of the measurement point from the Earth's centre of mass), and the Bouguer correction (eliminates the gravity effect of the rock mass between the observation point and the datum). These corrections are applied relative to a vertical datum, commonly sea level. The difference between the corrected gravity observation and the theoretical value of gravity on the reference ellipsoid at the observation point is known as the Bouguer gravity anomaly, which is the gravity parameter most commonly displayed on gravity maps.

Airborne Survey Specifications and Instrumentation

Airborne surveys are normally flown in a direction perpendicular to the main geological strike of the survey area. Line spacing depends on the objectives of the survey: in regional surveys, it commonly varies between 400 m and 1 km, whereas in detailed surveys flown for mineral exploration it may be as little as 100 or 200 m. Flight elevation in fixed-wing airborne surveys with magnetic and electromagnetic sensors varies typically from 150 to 300 m for regional surveys, and is about 100 m for detailed surveys. The flight elevation in fixed-wing surveys that include gamma-ray spectrometry is normally 120 m, although it may vary between 100 and 150 m. In the case of helicopter-borne surveys, the flight elevation is generally lower, at around 60 m, and the magnetic and electromagnetic sensors are suspended by cables at elevations of 45 and 30 m above ground, respectively. For helicopter-borne surveys with gamma-ray spectrometry, the detectors are mounted in the helicopter and the nominal terrain clearance varies between 60 and 90 m, depending on local terrain conditions and the configuration of other survey equipment. Differential GPS navigation is used, and the estimated accuracy of the flight path is better than 10 m. A vertically mounted video camera is normally used for verification of the flight path.

Magnetometer System

Split-beam cesium vapour magnetometers, having a sensitivity of 0.005 nT, are commonly used for magnetic surveying. Magnetic data are recorded every 0.1 second. The

magnetic data collected along the survey lines and the control lines are corrected for temporal (diurnal) variations in the magnetic field using ground-station magnetometer data. After editing the survey data, differences in magnetic values between traverse and control lines, established at intersections, are computer-analysed to obtain the levelling network. The magnetic data are then interpolated to a square grid having a dimension equal to approximately a quarter of the line spacing.

Electromagnetic System

Electromagnetic (EM) systems are either frequency-domain or time-domain systems. In Canada, frequency-domain surveys are flown with a helicopter. Time-domain systems can be operated in a helicopter or a fixed-wing aircraft. Line spacing usually ranges from about 100 to 250 m. As previously noted, when using a helicopter, the EM system is positioned at a height of approximately 30 m above ground. For fixed-wing systems, the plane and the transmitter fly at 120 m above ground, and the towed receiver is 50 m above ground.

Gamma-Ray Spectrometric System

A typical gamma-ray system includes a 256 channel spectrometer sampling data at 1 second intervals. Surveys flown with a fixed-wing aircraft usually consist of 50 litres of NaI(Tl) crystals in the main detector array with between 8 and 12 litres of NaI(Tl) crystals in the upward-looking detector array. Surveys flown using a helicopter will usually consist of 33 litres of NaI(Tl) crystals in the main detector array with 8 litres in the upward-looking array. After energy calibration of the spectra, counts from the main detector are recorded in five windows corresponding to thorium (2410-2810 keV), uranium (1660-1860 keV), potassium (1370-1570 keV), total radioactivity (400-2815 keV), and cosmic radiation (3000-6000 keV). Radiation in the upward-looking detector is recorded in a radon window (1660-1860 keV). Comprehensive descriptions of airborne and ground gamma-ray spectrometry surveying including fundamentals, instrumentation, calibration, data processing, and interpretation are covered by Grasty et al. (1991), Grasty and Minty (1995), Shives et al. (1995), Dickson and Scott (1997), Horsfall, (1997), Minty (1997), Minty et al. (1997), Wilford et al. (1997), and the International Atomic Energy Agency (2003) and references therein.

Mineral Deposit Types

Geophysical signatures are presented and discussed for nine major mineral deposit types: diamonds, lode Au, volcanogenic massive sulphides (VMS), sedimentary exhalative (SEDEX) base metals, Mississippi Valley-type (MVT) Pb-Zn deposits, porphyry Cu, unconformity-related U, Olympic Dam-type Cu-Au-Fe oxides, and magmatic Ni-Cu-PGE deposits. Comprehensive descriptions of these deposit types are included elsewhere in this volume (Corriveau, 2007; Dubé and Gosselin, 2007; Dubé et al., 2007; Eckstrand and Hulbert, 2007; Galley et al., 2007; Goodfellow and Lydon, 2007; Jefferson et al., 2007; Kjarsgaard, 2007; Paradis et al., 2007; Sinclair, 2007). The locations of deposits whose signatures are illustrated are plotted in Figure 9.

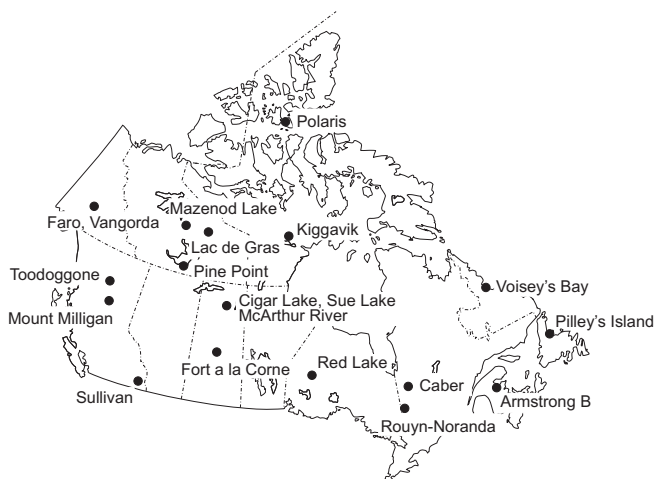


FIGURE 9. Locations of ore deposits for which geophysical signatures are illustrated.

Diamonds

Diamonds have been observed in a variety of geological environments, but typically only diamond-bearing kimberlites and lamproites, and paleoplacer and placer deposits derived from them are economic (Kjarsgaard, 1996, 2007; LeCheminant and Kjarsgaard, 1996). Typically kimberlites occur as inverted cone-shaped diatremes or pipes. These are the principal exploration targets and will be the focus of much of the following discussion. Hoover and Campbell (1992) reported that kimberlites range in diameter from 100 to 5000 m, but are generally 400 to 1000 m in diameter, and have a depth extent of about 2000 m. In Canada, in the Slave Province on the BHP/Dia Met property, most of the kimberlites have diameters of less than 400 m (St. Pierre, 1999). In the Kirkland Lake area, kimberlites with maximum widths of less than 400 m have been reported by Brummer et al. (1992). Larger diameters have been documented in the James Bay Lowlands, ranging from 50 to 1500 m (Reed, 1993).

Many kimberlites are associated with distinct circular magnetic anomalies that are related to magnetite produced by deuterian alteration of olivine (Mitchell, 1986). Iron-rich ilmenite (FeTiO_3) has a magnetic susceptibility ranging from about 2 to 3800×10^{-3} SI (Hunt et al., 1995). Presumably the significant magnesium contents of ilmenites in kimberlites would result in lower susceptibilities, but the authors are not aware of any published values for such ilmenites. The primary magnetic mineral in the BHP/Dia Met kimberlites in the Slave Province is reported to be titanomagnetite (St. Pierre, 1999), which has a susceptibility of 130 to 620×10^{-3} SI (Hunt et al., 1995). Katsebe and Kjarsgaard (1996) presented susceptibility values for Canadian kimberlites located in the Northwest Territories, Saskatchewan, and Ontario and indicated a range from about 1 to 100×10^{-3} SI. Clearly many kimberlites would produce positive magnetic anomalies, particularly where the host is sedimentary. In crystalline terrains, the sign of the anomaly would depend on the magnetic susceptibility of the host rocks.

A complication with respect to the expected sign of the magnetic anomaly is the presence of remanent magnetization, which may result in no magnetic anomaly or a negative

anomaly (Hoover and Campbell, 1992), a situation observed with respect to kimberlites on the BHP/Dia Met property in the Slave Province, where significant components of remanent magnetization are evident (St. Pierre, 1999). Inspection of a detailed survey flown at a height of 120 m along lines spaced 250 m apart in the Lac de Gras area (Shives and Holman, 1995) reveals that about 20% of the kimberlite bodies produce no obvious magnetic response, whereas the responses of the remainder may be divided into approximately equal numbers of positive and negative responses. The variability in magnetic signatures in this area is illustrated in Figure 10A (e.g. the Leslie kimberlite has a positive signature, whereas the Grizzly pipe has a negative response). St. Pierre (1999) stated that the Grizzly pipe (Fig. 10B) has a strong negative remanent component. The Lac de Gras area is also covered by a regional survey flown at a height of 300 m along lines spaced 800 m apart, and in this case only 10% of the known kimberlites can be visually identified in the magnetic data. This shows the importance of flying high-resolution magnetic surveys when exploring for kimberlites. Such surveys are often flown at a line spacing of 100 m. Another factor influencing the signature is possible variability of susceptibility within a single pipe (Keating, 1996). Whether positive or negative, magnetic anomalies associated with kimberlites can be expected to be circular to oval-shaped, mimicking the cross-section shape of the kimberlite. Keating (1996) has noted that most aeromagnetic signatures of kimberlites in the Canadian Shield are circular, though ground surveys define more complex anomalies, which may be elongated and/or contain internal highs. An automatic method for detecting such circular anomalies related to kimberlites has been developed by Keating (1995).

Electromagnetic responses of kimberlites are generally associated with crater facies, which includes epiclastic rocks that may contain shales and mudstones, or with altered (weathered/metasonitized) near-surface parts of diatremes that contain secondary serpentine, calcite, dolomite, chlorite and clay minerals (Mitchell, 1986). The kimberlite is identified by the higher conductivity of the fine-grained sedimentary rocks and component clay minerals, which contrasts significantly with generally more resistive host rocks. Good examples of strong conductivity responses are observed in the Fort à la Corne area (Fig. 10D). St. Pierre (1999) reports that crater facies material in the BHP/Dia Met field has resistivities as low as 0.5 Ohm-m, which compares with typical resistivities of several thousand Ohm-m for hosting granites and gneisses. Because kimberlites in the Northwest Territories are generally located under lakes or swamps it may be difficult to determine if the observed EM response is due to the kimberlite itself, or to the increased thickness of the conductive overburden. However, some EM anomalies are clearly associated with the pipe itself; examples from the Lac de Gras area are presented by Smith et al. (1996). In the Kirkland Lake area, there are no EM anomalies associated with known kimberlites, nevertheless an increase of the conductivity due to a thicker conductive overburden is observed (Keating, 1995). Resistivities of Canadian kimberlites, published by Katsebe and Kjarsgaard (1996), indicate a marked dichotomy, with values ranging from approximately 10 to 1000 Ohm-m, for crater and diatreme facies and from roughly 1000 to 100000 Ohm-m for hypabyssal facies.

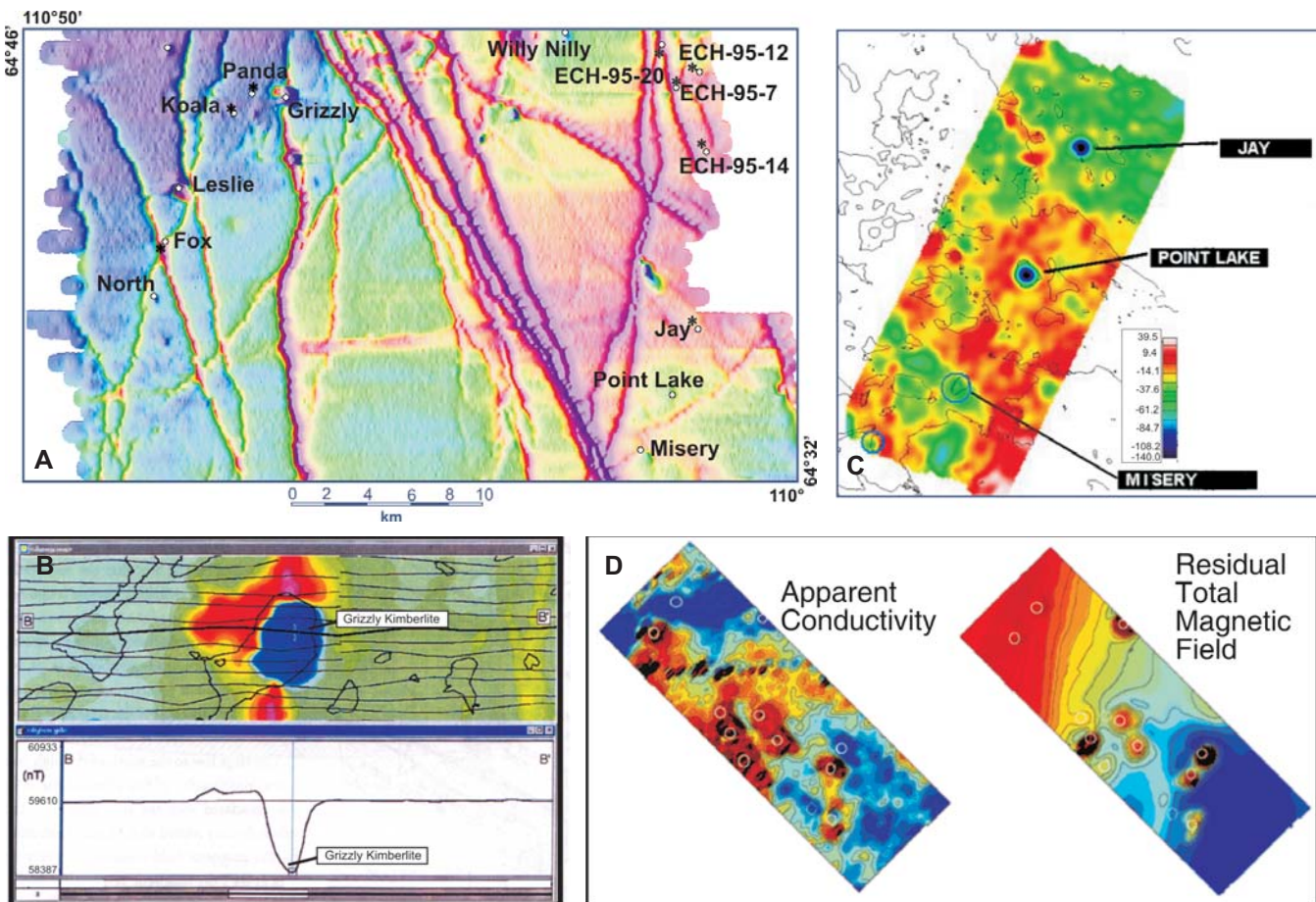


FIGURE 10. (A) Total magnetic field signatures of some kimberlite bodies in the Lac de Gras area. The flight elevation was 120 m and the line-spacing 250 m; (B) Negative total magnetic field anomaly over the Grizzly pipe, Lac de Gras area; flight elevation 30 m, flight-line spacing 125 m (adapted from St. Pierre, 1999); (C) Vertical gravity gradient from an airborne survey, Lac de Gras area (image from www.bhpbilliton.com); (D) Apparent conductivity and residual total magnetic field, Fort à la Corne area (image from www.fugroairborne.com). In all cases, the fields are represented by colour schemes that go from low values (blue shades) to high values (red shades).

Of significance to geophysical detection are the high densities of most minerals. Kjarsgaard's (1996) description of the mineralogical composition of kimberlites notes the inequigranular texture consequent on the presence of large macrocrysts and phenocrysts within a fine-grained matrix. Macrocrysts include the minerals olivine (density = 3.27–4.37 g/cm³), Mg-ilmenite (4.7 g/cm³), Ti-Cr-pyrope garnet (3.51 g/cm³), clinopyroxene (3.2–3.3 g/cm³), phlogopite (2.86 g/cm³), enstatite (3.2–3.5 g/cm³), and zircon (4.68 g/cm³). Primary matrix minerals include olivine and a variety of minerals with densities that range between 2.2 g/cm³ for primary serpentine and 4.7 g/cm³ for ilmenite. The high densities of these minerals have the potential to create positive gravity anomalies, although this is tempered by the presence of the low density serpentine, which may have an overriding influence and produce negative anomalies. In fact, Hoover and Campbell (1992) reported that gravity anomalies associated with kimberlites are generally negative (of the order of 1 mGal amplitude), as a result of serpentization and weathering of the constituent mafic rocks. In the Slave Province, St. Pierre (1999) noted mean densities of 1.9, 2.2, and 2.9 g/cm³ for crater, diatreme, and hypabyssal facies, respectively, of several kimberlites. Contrasted against a mean background density of 2.7 g/cm³ of hosting

granites and gneisses, these values indicate the potential for both negative and positive gravity anomalies. However, since most kimberlites in the area comprise crater and diatreme facies, negative gravity anomalies prevail. In the Fort à la Corne area, kimberlites have a positive gravity signature because they are hosted in lighter sedimentary rocks (Cretaceous shales).

Airborne gravity gradiometry surveys have been successful in delineating kimberlites in the Lac de Gras area. Distinct signatures were imaged over the Jay and Point Lake bodies, but the Misery kimberlite produced little signal (Fig. 10C).

Individual kimberlites exhibit a wide range of radioactive element concentrations (Mitchell, 1986). Variations in K₂O content reflect petrographic divisions between micaeous K₂O-rich (0.09–5.04%) and mica-poor kimberlites (0.02–2.15%). Uranium and thorium concentrations range between 0.5 and 22.9 ppm (mean = 3.1 ppm) and between 2.8 and 920 ppm (mean=17 ppm), respectively.

Airborne gamma-ray spectrometry signatures of kimberlites are not well documented. Hoover and Campbell (1992) and Richardson (1996) report that radioactive element surveys have not been effective in the search for kimberlites. However, Hoover and Campbell (1992) observed that several papers had reported on the use of radioelement surveys

in Yakutia, Russia for discriminating between diamond-bearing basaltic kimberlites and barren micaceous kimberlites and carbonatites. An airborne gamma-ray spectrometry survey flown over the Lac de Gras area (Shives and Holman, 1995) did not detect discernable radioactive element signatures over any of the known kimberlites. This was to be expected given that most pipes are located under lakes and swamps that mask any radiometric responses. Nevertheless, in other kimberlite districts it might be expected that significant radioactive element signatures would be detectable with better exposure. For example, kimberlite intruded into sedimentary sequences with low radioactivity, such as limestone, and not covered by lakes or otherwise water-saturated, could have a detectable radioactive element signature. Mwenifumbo and Kjarsgaard (2002) report that borehole gamma-ray spectrometry measurements, conducted in conjunction with other borehole logging techniques, have been particularly useful in defining different phases of kimberlite pipes.

On the ground, pipe delineation can be done using standard geophysical techniques. Magnetic surveys are used to define the internal structure of the pipe, and eventually identify different intrusion phases (Macnae, 1995). Gravity surveys are used to determine the 3-D architecture of a pipe and investigate its depth extent. In the Fort à la Corne area, ground gravity was used to determine the depth extent and geometry of a pipe (Lehnert-Tiel et al., 1992). In this case, the gravity anomaly is positive because the kimberlite is located within less dense Cretaceous shales. Induced-polarization and resistivity surveys can be used to map the altered top part of the pipe (e.g. Macnae, 1979).

Seismic surveys are useful as a follow-up exploration tool for defining the geometry and internal structure/stratigraphy of kimberlites. Gendzwill and Matieshin (1996) provide a Canadian example of a seismic study conducted on the Smeaton kimberlite in the Fort à la Corne field, Saskatchewan. Vertical seismic reflection profiling conducted along 13 line-km permitted a refinement of subsurface information revealed by drillholes, yielding information on the shape and extent of the kimberlite and its stratigraphic relationships. It also supports a picture of a crater facies emplaced by several explosive episodes with continuing sedimentation between these events.

Lode Gold Deposits

A lode Au deposit is a hydrothermal deposit whose principal commodity is Au. Dubé and Gosselin (2007) provide a comprehensive synthesis of this deposit type and its various subcategories including 1) shear- and fault-zone-related deposits, principally greenstone-hosted quartz-carbonate vein deposits (orogenic, mesothermal, lode gold, shear-zone-

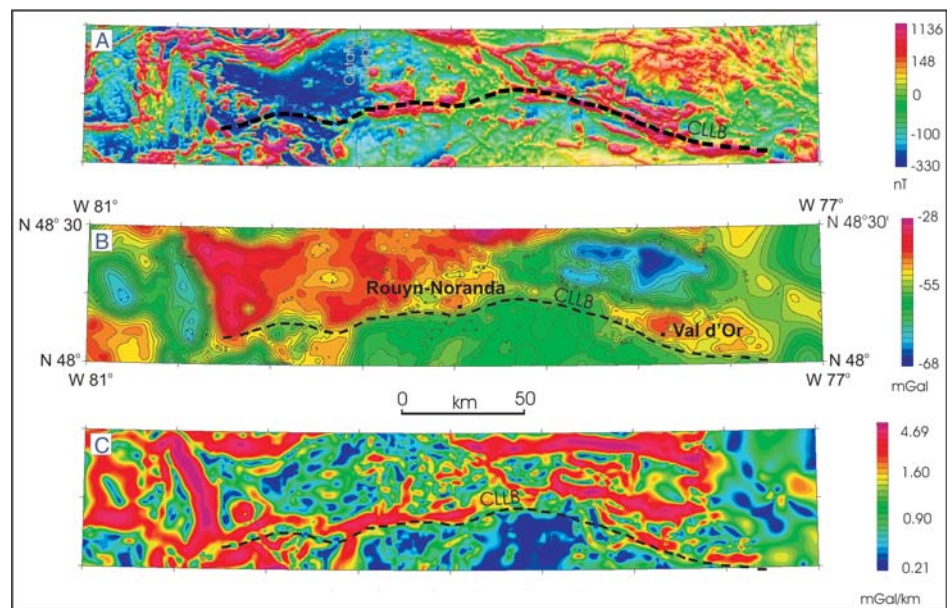


FIGURE 11. The Cadillac-Larder Lake Break (CLLB) superposed on (A) total magnetic field map; (B) Bouguer gravity anomaly map; and (C) a map of the horizontal gradient of the Bouguer gravity anomaly

related quartz-carbonate or gold-only deposits) associated with collisional tectonics, 2) intrusion-related deposits associated with felsic plutons of subaerial, oceanic, and continental setting, and 3) epithermal deposits (high- and low-sulphidation) associated with subaerial and shallow-marine environments (Lydon et al., 2004).

Shear- and fault-zone-related deposits are a major source of world gold production and represent about a quarter of Canada's production (Ash and Alldrick, 1996). Major Canadian examples include a number of deposits in the Timmins, Kirkland Lake, Red Lake, and Val D'or mining camps. Dubé and Gosselin (2007) describe these deposits as simple to complex networks of gold-bearing, laminated quartz-carbonate fault-fill veins. They are typically hosted by greenschist- to locally amphibolite-facies metamorphic rocks of predominantly mafic compositions. They occur near major compressional faults, but are usually localized along associated second-order faults and splays. Narrow zones (<1 m) of silicification, pyritization, and potassium metasomatism occur within broader zones (10s of metres) of carbonate alteration.

Low-sulphidation epithermal deposits are described by Panteleyev (1996a) as Au- and Ag-bearing quartz veins, stockworks, and breccias that exhibit open-space filling textures and are associated with volcanic-related hydrothermal and geothermal systems. High-sulphidation deposits occur as veins, vuggy breccias, and sulphide replacements associated with epizonal hydrothermal systems characterized by acid-leached, argillic, and siliceous alteration (Panteleyev, 1996b). Minerals relevant to geophysical detection include pyrite, sericite/illite, alunite, adularia, kaolinite, muscovite, magnetite, pyrrhotite, quartz, and carbonate minerals.

A variety of geophysical techniques are applicable to Au exploration. Specific methods will depend on lithological, mineralogical, and alteration characteristics of each deposit type. In general, for shear- and fault-zone (Au-quartz vein) deposits aeromagnetic data can provide valuable mapping

Overview of Geophysical Signatures Associated with Canadian Ore Deposits

TABLE 3. Massive sulphide ore mineral density (g/cm^3) and magnetic susceptibility (10^{-3} SI).

Mineral	Density	Susceptibility
Barite	4.5	?
Chalcopyrite	4.2	0.4
Pyrite	5.02	5
Pyrrhotite	4.62	3200
Sphalerite	4	0.8
Galena	7.5	-0.03
Magnetite	5.18	5700
Hematite	5.26	40

Densities from Klein and Hurlbut (1985)

Susceptibilities from Hunt et al. (1995)

information by delineating lithologies, regional faults, and shear zones. An excellent example is the Cadillac Larder Lake Break (CLLB) in the Archean Abitibi belt, which extends for more than 200 km in an east-west direction. This major fault zone is characterized by the presence of numerous gold deposits. Although gold deposits have no geophysical response, the structures controlling gold mineralization may produce distinct geophysical signatures. Figure 11A, derived from the archives of the Geological Survey of Canada's Geophysical Data Repository, shows the residual total magnetic field in the area. The CLLB (black dotted line) is marked by a series of linear magnetic anomalies generally located on its north side. Figure 11B shows the Bouguer gravity anomaly over the same area. Data spacing is highly variable, between 500 m and over 10 km. Nevertheless, the CLLB is easily identifiable over most of its length. It is even easier to locate in Figure 11C, which displays the magnitude of the horizontal gradient of the Bouguer gravity anomaly used to map contacts between units of different densities.

At deposit-scale, magnetic lows can delineate areas of magnetite destruction associated with carbonate alteration. EM methods have also been used to map faults, veins, contacts, and alteration. IP methods and gamma-ray spectrometry may have local applications to map massive quartz veins (resistivity highs) and associated alteration (e.g. potassium highs (Shives et al., 1995)).

Klein and Bankey (1992) note that for epithermal styles of mineralization several types of geophysical signatures have been used to delineate favourable geology, structures, and alteration. These include regional-scale gravity lows that define favourable, thick, silicic volcanic sequences, or long-wavelength magnetic lows that are associated with alteration. Regional resistivity lows may be associated with weathered and altered volcanic sequences. Klein and Bankey (1992) state that while there are no geophysical signatures to directly detect epithermal vein mineralization, favourable deposit-scale structures and alteration can be measured. Gravity signatures are variable, ranging from highs associated with subvolcanic intrusions or structural highs within volcanic sequences to local gravity lows associated with zones of brecciation or fracturing. Alteration may result in local magnetic lows. Potassium highs are to be expected due to K alteration. However, naturally high K rock-types in the vicinity of mineralization may make identification of K enrichment associated with mineralization difficult. Low

eTh/K ratios may be a more sensitive indicator of alteration (Shives et al., 1997). Resistivity lows may occur with associated sulphide mineralization, argillic alteration, and increased porosity related to open brecciation. However, resistivity highs will occur in zones of silicification or associated with intrusions or basement uplifts (Klein and Bankey, 1992). Associated pyritic alteration may cause high IP anomalies.

Some of these geophysical signatures are illustrated in Figure 12. In the Red Lake area, K enrichment is known to occur along the Madsen-Starrett-Olsen shear zone (Durocher, 1983) related to gold mineralization. Figure 12 shows results from a detailed, 250 metre line spaced, airborne gamma-ray spectrometry and total field magnetic survey (Hetu, 1991). The Madsen-Starrett-Olsen Zone shows a weak but distinct K anomaly that is unusual considering the underlying mafic volcanic lithologies. Higher amplitude K anomalies occur over granitic and felsic metavolcanics to the south and west. The K enrichment associated with the mineralized zones can be differentiated from the high K concentrations associated with the granitic and felsic metavolcanics by virtue of the fact that the mafic lithologies that host the mineralization have low Th concentrations. The associated K enrichment results in low eTh/K ratios. Similarly, in the Toodoggone area of British Columbia, a number of Au deposits and occurrences occur directly associated with or in close proximity to low eTh/K ratio anomalies.

Volcanogenic Massive Sulphide (VMS) Deposits

Volcanic massive sulphide (VMS) deposits form by discharge of hydrothermal solutions onto the seafloor, commonly near plate margins. A comprehensive synthesis of VMS deposits is provided by Galley et al. (2007). VMS deposits typically develop in the form of a concordant lens that is underlain by a discordant stockwork or stringer zone comprising vein-type sulphide mineralization located in a pipe of hydrothermally altered rock.

VMS deposits typically have density, magnetic, conductivity, and acoustic velocity properties that differ significantly from those of their host rocks. There is, therefore, enormous potential for direct detection of orebodies using geophysical methods that measure these properties. The most common sulphide mineral in VMS deposits is pyrite, which may be accompanied by subordinate pyrrhotite, chalcopyrite, sphalerite, and galena (Galley et al., 2007). Magnetite, hematite, and cassiterite are common nonsulphide metallic minerals, and the gangue mineral barite may also be present. Densities of these minerals range from 4.0 to $7.5 \text{ g}/\text{cm}^3$ (Table 3). Singularly or in combination, these minerals will have a large density contrast with respect to densities of host sedimentary and volcanic rocks; some typical values in the Bathurst Mining Camp range from 2.70 to $2.84 \text{ g}/\text{cm}^3$ (Thomas, 2003). Mean densities of massive to semimassive sulphides measured on drill core from several deposits in the Bathurst Mining Camp are naturally less than individual mineral densities, but nevertheless range from 3.58 to $4.42 \text{ g}/\text{cm}^3$ (Thomas, 2003). Most deposits in the Camp generate distinct gravity highs, the largest being associated with the Brunswick No. 6 deposit measured at approximately 4.0 mGal in amplitude prior to mining (Thomas, 2003).

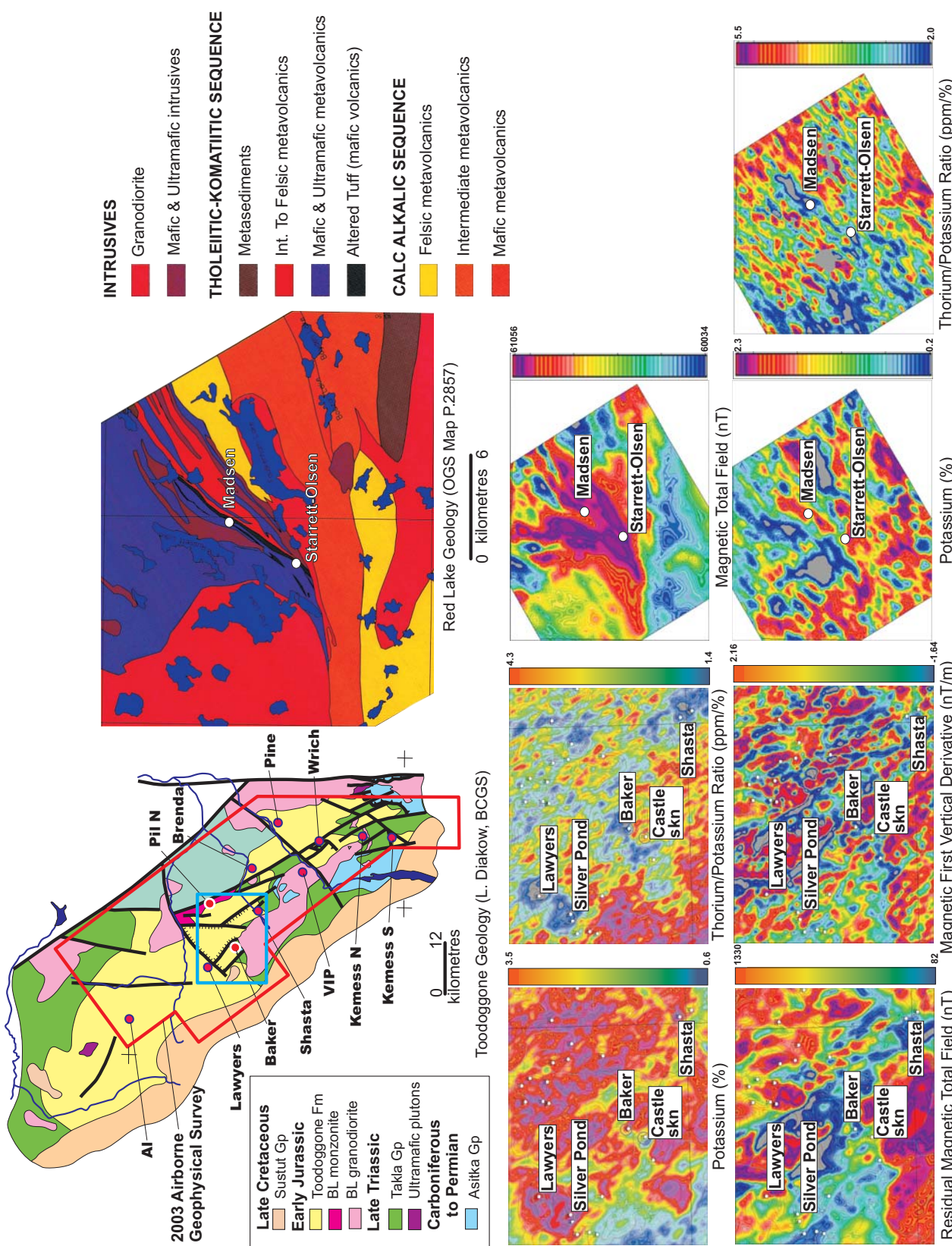


FIGURE 12. Airborne gamma-ray spectrometric and magnetic signatures over gold mineralization in the Toodoggone area, British Columbia (from Shives et al., 2004) and Madsen-Starrett-Olsen Zone, Red Lake area, Ontario (Hetu, 1991). In both examples, detailed structural information is provided by both the aeromagnetic and gamma-ray spectrometric data, and K enrichment due to alteration associated with mineralization is differentiated from high K lithologies by corresponding low Th/K ratios. White dots represent known mineralization.

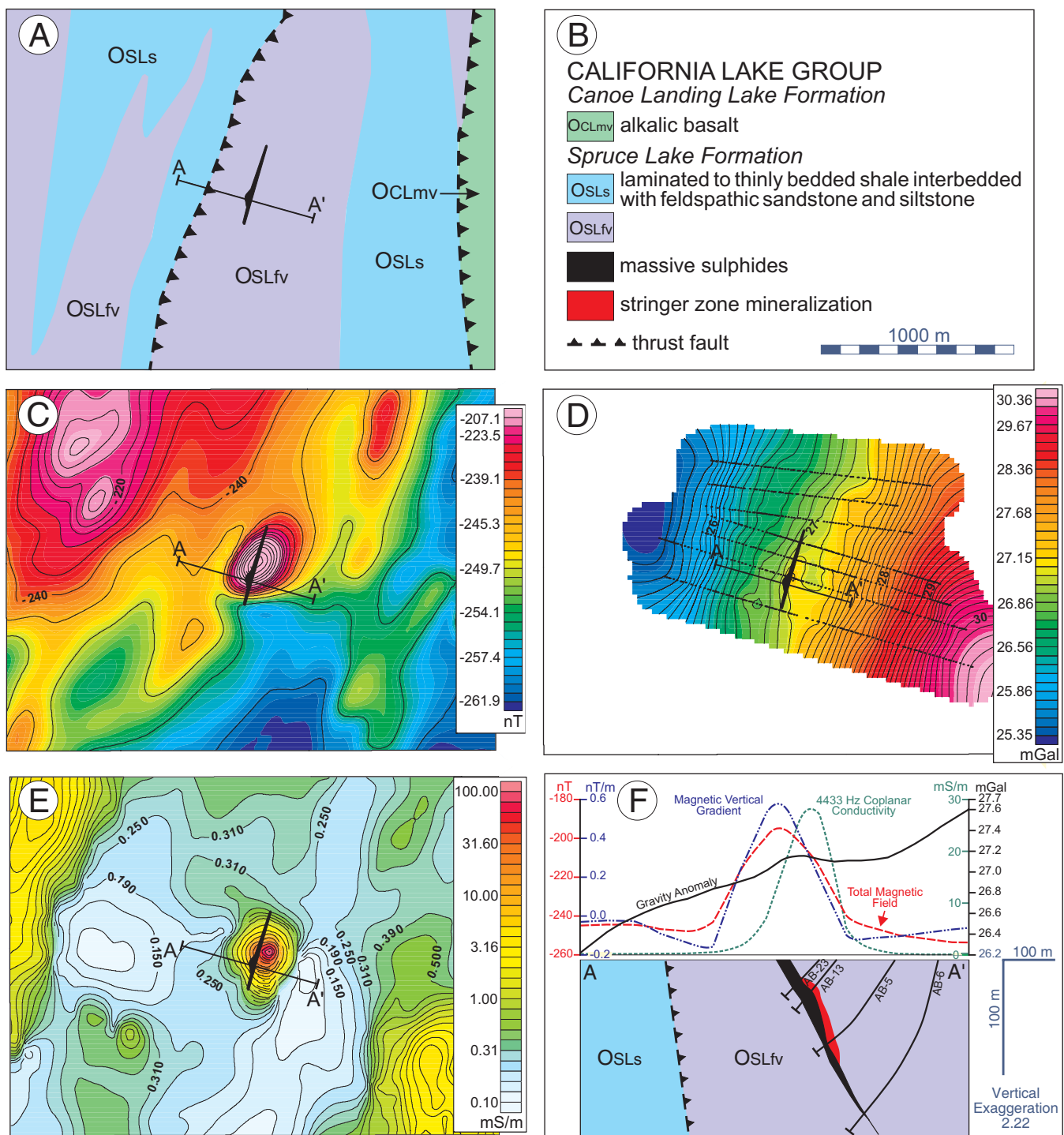


FIGURE 13. Geological and geophysical maps of the area containing the Armstrong B massive sulphide deposit, Bathurst mining camp, New Brunswick, together with geophysical profiles across the deposit. **(A)** Geological map (after van Staal, 1994); **(B)** Geological legend; **(C)** Map of magnetic field; **(D)** Map of gravity anomalies; **(E)** Map of conductivity (4433 Hz frequency; coplanar transmitter-receiver); and **(F)** Total magnetic field, vertical magnetic gradient, gravity anomaly, and conductivity (4433 Hz; coplanar) profiles crossing the Armstrong B deposit. The foregoing panels are based on images published by Thomas et al. (2000).

High magnetic susceptibilities of most sulphide minerals, except sphalerite and galena, ensure that prominent magnetic anomalies are also associated with VMS deposits. Bishop and Emerson (1999) note that sphalerite has no salient geochemical properties allowing its direct routine detection by geophysics. They note further that even though sphalerite occurs along with other detectable sulphides, detection of

Zn-bearing deposits is very difficult. Pyrrhotite has the largest magnetic susceptibility (3200×10^{-3} SI) of the sulphide minerals and its presence is important to the detection of the sulphide body. Pyrite is by far the most common sulphide mineral in a sulphide lens (Galley et al., 2007) and has a susceptibility of 5×10^{-3} SI, which is considerably larger than susceptibilities (0.1 to 1.1×10^{-3} SI) of most host sediments.

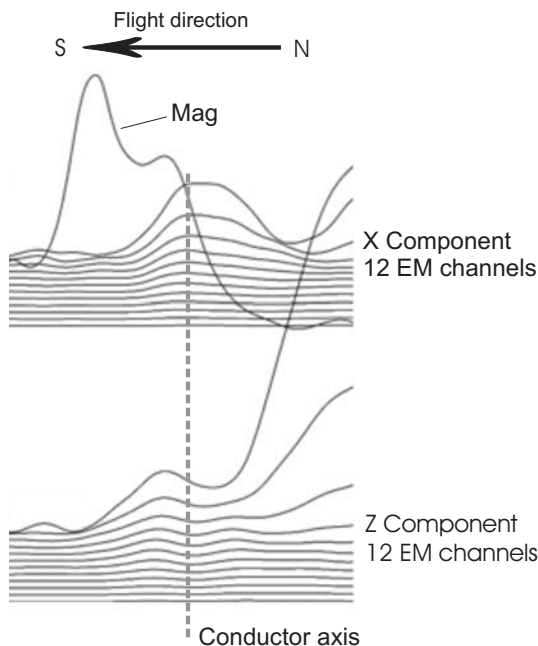


FIGURE 14. Electromagnetic (GEOTEM) profiles across the Caber volcanic massive sulphide deposit, 35 km west of Matagami, Quebec. Top channels are early time channels; the vertical scales are relative. There is an anomalous EM response on both the X and Z component. The higher amplitude, early time responses of the Z component are caused by a thickening of the overburden (~20 m) under the northern part of the profile. The profile is approximately 1 km long.

mentary and volcanic units in the Bathurst Mining Camp (Thomas, 1997). Thus, discernible positive signatures are expected over VMS deposits of significant size and should provide pointers to potentially economic mineralization because of the common association with chalcopyrite, sphalerite, or galena. Chalcopyrite and sphalerite have susceptibilities (Table 3) similar to those of sedimentary and volcanic hosts, and are unlikely to generate a strong magnetic signal. Galena, with a small negative susceptibility, also would have little influence on the magnetic field. Lydon (1984) observes that magnetite and hematite are two common nonsulphide metallic minerals occurring in sulphide lenses. For some VMS deposits, magnetite tends to be concentrated in the core of the stockwork and central, basal part of the overlying sulphide lens. The association of VMS deposits and magnetite, coupled with the large susceptibility of magnetite (5700×10^{-3} SI), provides a “remote” sensor for sulphide species via magnetic anomalies produced by magnetite. Hematite has a much smaller susceptibility (40×10^{-3} SI) than magnetite, but still has potential to produce sizable positive signals. Also of great importance in vectoring VMS deposits are temporally and spatially associated iron-formations, some of which contain magnetite (Peter et al., 2003), and produce prominent magnetic anomalies.

A comprehensive and illustrated description of gravity, magnetic, conductivity, and radiometric signatures for twenty sulphide deposits in the Bathurst Mining Camp, New Brunswick is presented by Thomas et al. (2000). Illustrations of geophysical signatures for the small Armstrong B VMS deposit are shown in Figure 13. The time-domain airborne EM signature (GEOTEM) for the Caber VMS deposit located west of Matagami, Quebec, obtained subsequent to

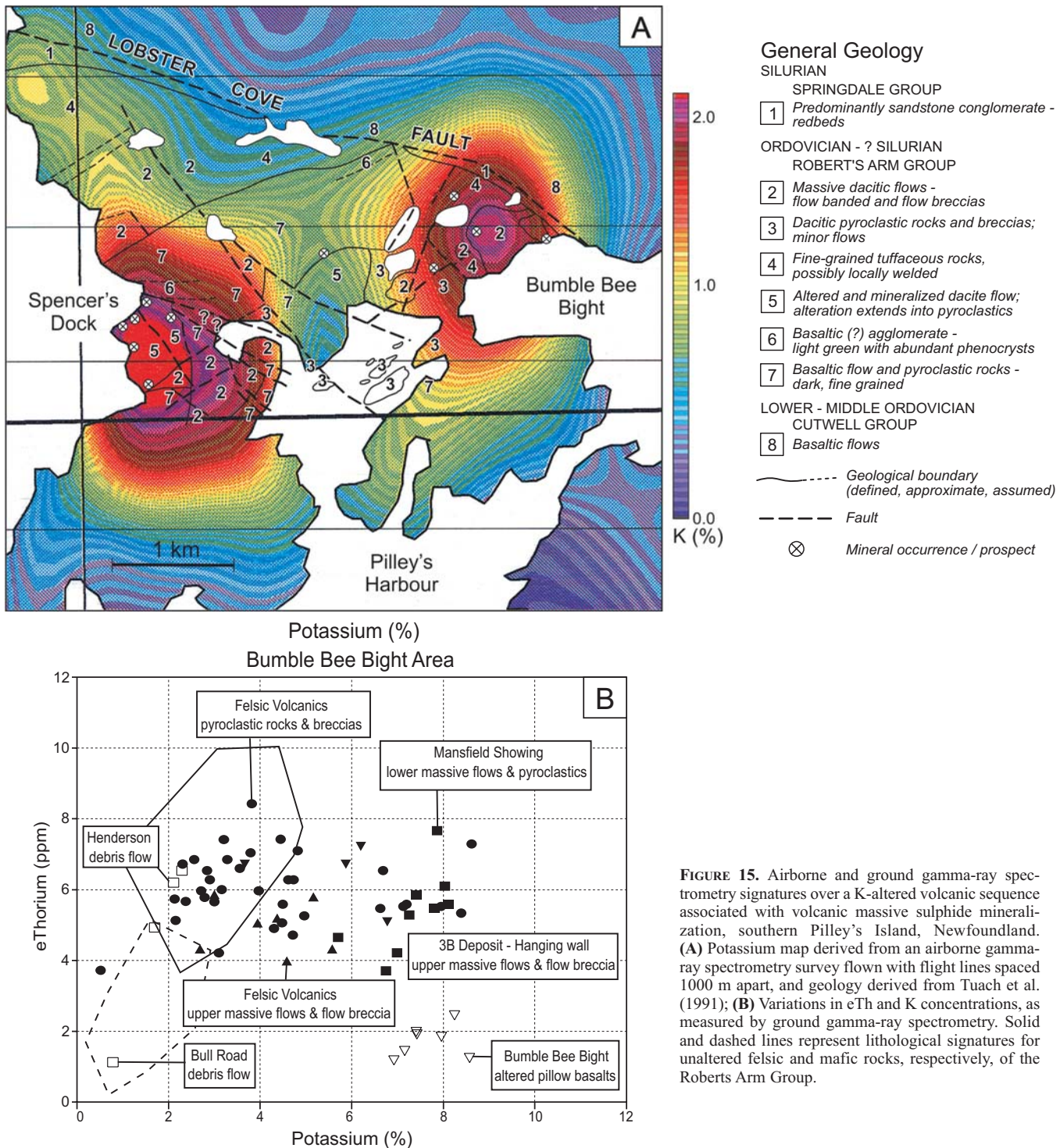
discovery, is shown in Figure 14. This copper-zinc deposit, containing 1.3 MT at 1.3% Cu and 5.5% Zn, was discovered by BHP Minerals Canada in 1994. The deposit is located on the Key Tuffite horizon, along which are located the base metal VMS deposits of the Matagami Mining Camp. The strike length of the deposit is 200 to 250 m with a down-dip extent of 150 to 250 m. Bedrock is overlain by approximately 20 m of conductive overburden. Strong airborne and ground gamma-ray spectrometry signatures over K-altered mafic and felsic volcanic rocks associated with a massive sulphide deposit at Pilley’s Island, Newfoundland (Shives et al., 1997) are shown in Figure 15.

SEDEX Base Metals Deposits

Sedimentary exhalative (SEDEX) sulphide deposits are found in sedimentary basins, usually in the form of conformable to semiconformable sheets or tabular lenses of stratiform sulphides (Lydon, 1995; Goodfellow and Lydon, 2007). Such bodies have typical aspect ratios of 20, maximum thicknesses of 5 to 20 m (Lydon, 1995), and may extend over a distance of more than 1 km (Goodfellow and Lydon, 2007). The principal ore minerals are sphalerite and galena. Chalcopyrite is sometimes concentrated in feeder zones of SEDEX deposits, but only rarely attains concentrations of economic interest. Pyrite is the most abundant sulphide, and pyrrhotite may be common.

The physical and chemical properties of SEDEX deposits make them amenable to detection by several geophysical techniques. In the Purcell Basin, southeastern British Columbia, sulphide mineralization associated with the Sullivan and smaller North Star and Stemwinder Pb-Zn-Ag deposits is reflected by strong finite conductors and positive magnetic anomalies (Fig. 16) (Lowe et al., 2000). Conductors coinciding with the western margin of the Sullivan deposit, where it is cut by the Sullivan fault, are attributed to an uneconomic massive pyrrhotite body underlying the western and shallowest part of the underground workings. A magnetic high associated with the deposit is also explained by this same body. Elevated K values and depleted eTh/K ratios, relative to those of unmineralized host rocks in the Sullivan-North Star corridor (Fig. 16), are associated with areas of hydrothermal sericitic alteration.

In the Anvil district, Yukon, a combination of magnetic, electromagnetic, and gravity methods detected the Vangorda, Faro, and Swim Lake deposits (Brock, 1973), with significant geophysical signatures being recorded over each deposit, though not necessarily for each method in every case. The Faro deposit was associated with a positive gravity anomaly more than 2.5 mGal in amplitude and a magnetic anomaly of about 300 nT amplitude (Figs. 17, 18). The Vangorda deposit also produced significant gravity and magnetic anomalies, having amplitudes of about 2 mGal and 800 nT, respectively (Fig. 19). Airborne electromagnetic surveys using a vertical coaxial transmitter-receiver configuration operating at 4000 Hz recorded strong in-phase responses from the Vangorda (up to 120 ppm) and Swim (190 ppm) deposits, but only weak to moderate responses over the Faro No. 1 (19 ppm) and Faro No. 2 (41 ppm) deposits (Brock, 1973).



Mississippi Valley-Type Lead-Zinc Deposits

Mississippi Valley-type (MVT) Pb-Zn deposits are typically stratabound, some are prismatic pipe-shaped bodies, hosted by limestone or dolomite in platform carbonate sequences (Sangster, 1995) and occur in clusters. Sphalerite and galena are the dominant ore minerals that characteristically occupy open spaces in carbonate breccias; replacement of host rocks is relatively rare. Most deposits or MVT districts occur below unconformities or nonconformities,

related probably to minor uplift or warping, but few deposits have been affected by subsequent deformational events. Dimensions of the one hundred known orebodies in the Pine Point district vary from 60 to 2000 metres in length, 15 to 1000 metres in width, and 0.5 to 100 metres in thickness (Hannigan, 2007). Additional information on various aspects of MVT deposits may be found in Dewing et al. (2007), Hannigan (2007), Paradis and Nelson (2007), and Paradis et al. (2007).

FIGURE 16. Geophysical images of the Sullivan - North Star area. Crossed-hammer symbols mark the centre of the Sullivan deposit in the north and the North Star deposit in the south. Dashed line shows the vertical projection of the economic limit of the Sullivan orebody. (A) EM (apparent conductivity estimated from 900 Hz coaxial data). Locations of calculated cultural and noncultural finite conductors are indicated by open and solid circles, respectively (conductivity values range from 0 to 5800 mS/m); (B) Magnetic anomalies (values range from -40 nT to +80 nT); (C) Potassium levels (values range from 0.86-2.83%); and (D) eTh/K ratios (values range from 3.09 to 6.99). In all cases, hot colours indicate high values and cool colours indicate low values. Information from Lowe et al. (2000).

The generally concentrated nature of the mineralized zones, high densities of sphalerite and galena, high conductivity of galena, and significant conductivities of commonly associated sulphides, such as pyrite, marcasite, and pyrrhotite, make the induced polarization (IP) and gravity methods the favoured approaches for exploration. At Pine Point, Seigel et al. (1968) attributed the discovery of the two Pyramid orebodies to time-domain IP surveys, with a subsequent gravity survey credited with focusing a drilling program and contributing to tonnage estimations. Distinct gravity (>0.8 mGal amplitude, Fig. 20) and chargeability (~ 21 ms, Fig. 21) anomalies were mapped over the tabular Pyramid No. 1 body. Turam electromagnetic data shows no discernable response, presumably due to the disconnected nature of marcasite common in the Pine Point deposit.

Lajoie and Klein (1979) also reported success with the IP and gravity methods in the Pine Point district, noting again the lack of electromagnetic responses, which was ascribed generally to calcite and dolomite gangue interrupting the conducting paths, though non-conductive and nonpolarizable sphalerite, the dominant mineral in the orebodies, plays a similar role. The IP method was considered the best exploration tool in this district, even for orebodies having small lateral dimensions, and the gravity method was regarded as an excellent complement to IP. The magnetic method may have some suc-

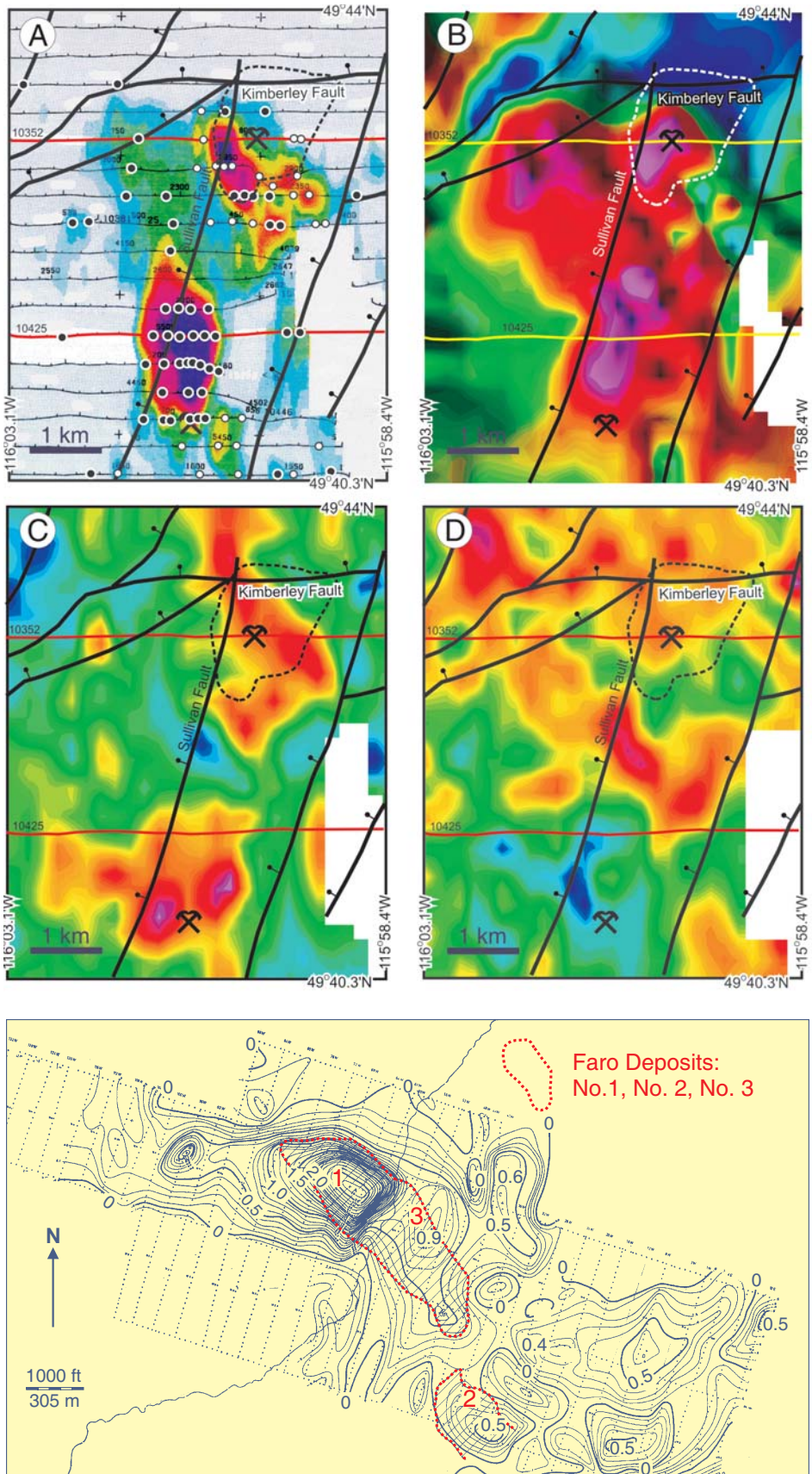


FIGURE 17. Residual Bouguer gravity anomaly map of the Faro SEDEX deposit, Yukon, which includes three separate orebodies, referred to as the No. 1, No. 2, and No. 3 deposits. This figure is a modified version of Figure 11 published by Brock (1973). Contour interval = 0.1 mGal.

Overview of Geophysical Signatures Associated with Canadian Ore Deposits

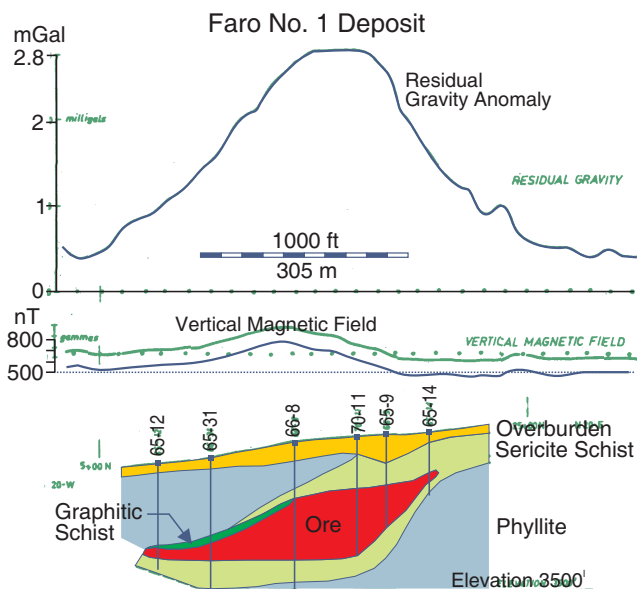


FIGURE 18. Bouguer gravity and vertical magnetic field profiles crossing the Faro No. 1 SEDEX deposit, Yukon (after Brock, 1973).

cess if the ore is associated with pyrrhotite, an example of a small, 20 nT amplitude magnetic anomaly coexisting with a small uneconomic mineralized body is illustrated (Fig. 22). Lajoie and Klein (1979) describe results of seismic reflection experimentation in the region, designed to assess the method's capability as a tool for mapping, for finding ores directly and for outlining structures associated with mineralization. A successful result was the delineation of a large collapse structure within the hosting clastic reef complex. This structure may have influenced the development of an ore-body located within it. In Nunavut, in the arctic islands, Hearst et al. (1994) reported on high-resolution seismic reflection profiling across the pyritic South Boundary Zone of the Nanisivik MVT deposit, concluding that sulphide mineralization could be detected to moderate depths of up to about 200 m if it had a minimum thickness of 5 to 10 m and

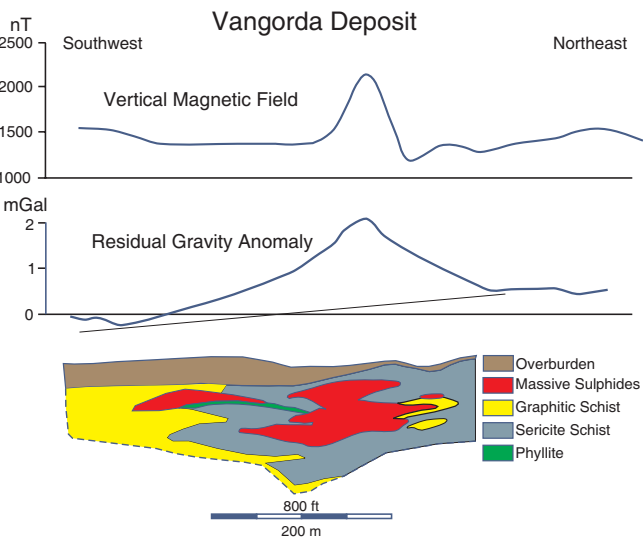


FIGURE 19. Bouguer gravity and vertical magnetic field profiles crossing the Vangorda SEDEX deposit, Yukon (after Brock, 1973).

a lateral extent on profile of at least 10 m. Also in the Arctic, the gravity method is credited with the discovery of the Polaris lead-zinc deposit, which produced an anomaly of about 0.9 mGal amplitude (Fig. 23).

Porphyry Copper Deposits

Porphyry deposits are a major source of production for Cu, Mo, and Re, and an important source for Au, Ag, and Sn. Sinclair (2007) provides a comprehensive synthesis of porphyry deposits. Porphyry-style base and precious metal mineralization is spatially and genetically related to high level, epizonal and mesozonal felsic to intermediate porphyritic intrusions and adjacent host rocks. Mineralization may be in the form of stockwork quartz veins and veinlets, fractures, disseminations, and replacements containing pyrite, chalcopyrite, bornite, and magnetite. Deposit forms are quite variable and range in size from hundreds to thousands of metres laterally and with depth, and are commonly zoned

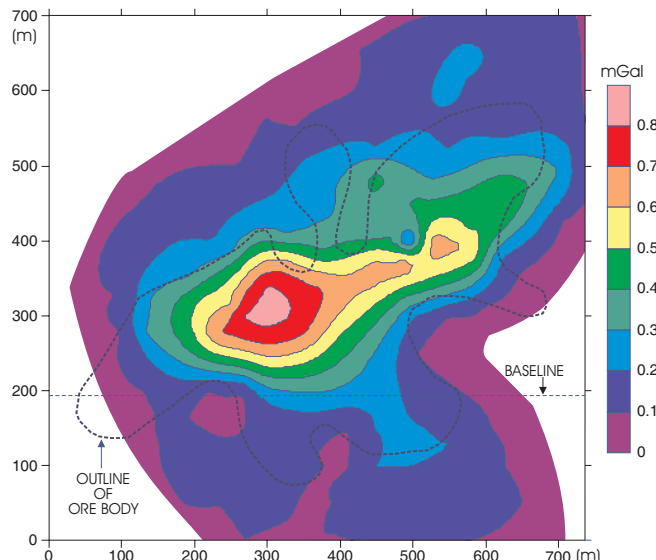


FIGURE 20. Bouguer gravity anomaly associated with the Pyramid No. 1 orebody, Pine Point District, Northwest Territories (after Seigel et al., 1968).

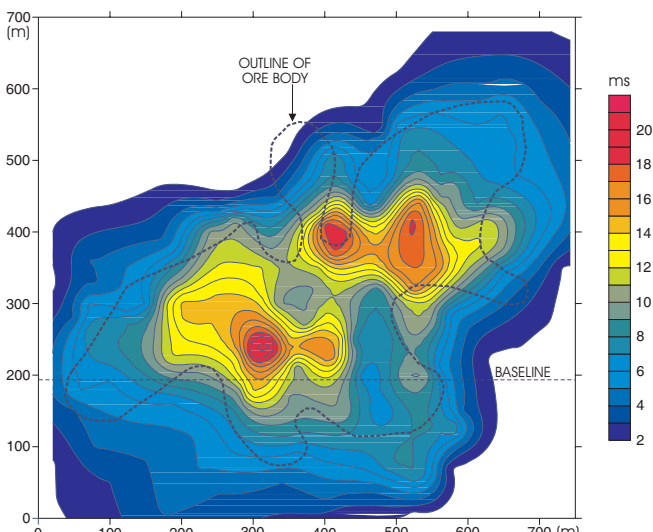


FIGURE 21. Chargeability anomaly associated with the Pyramid No. 1 orebody, Pine Point District, Northwest Territories (after Seigel et al., 1968).

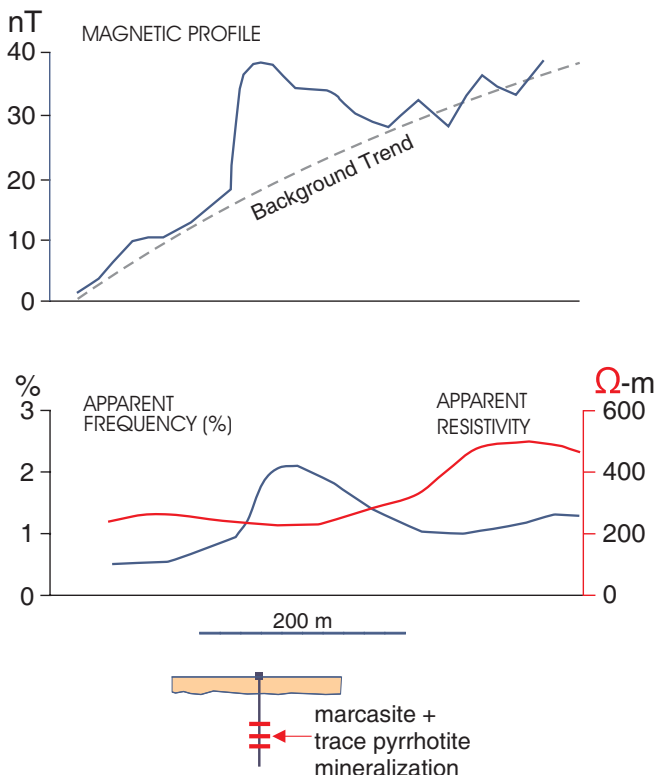


FIGURE 22. Magnetic, apparent resistivity and apparent frequency profiles crossing an uneconomic mineralized body, Pine Point District, Northwest Territories (after Lajoie and Klein, 1979).

with barren cores and generally concentric metal zones surrounded by barren pyritic haloes. Alteration associated with porphyry deposits is typically zoned from an inner potassic (biotite and/or K-feldspar) alteration zone, closely associated with mineralization, to a more extensive propylitic alteration zone consisting of quartz, chlorite, epidote, calcite, albite, and pyrite, which surrounds the inner potassic zone. Zones of phyllitic and argillic alteration may occur between and

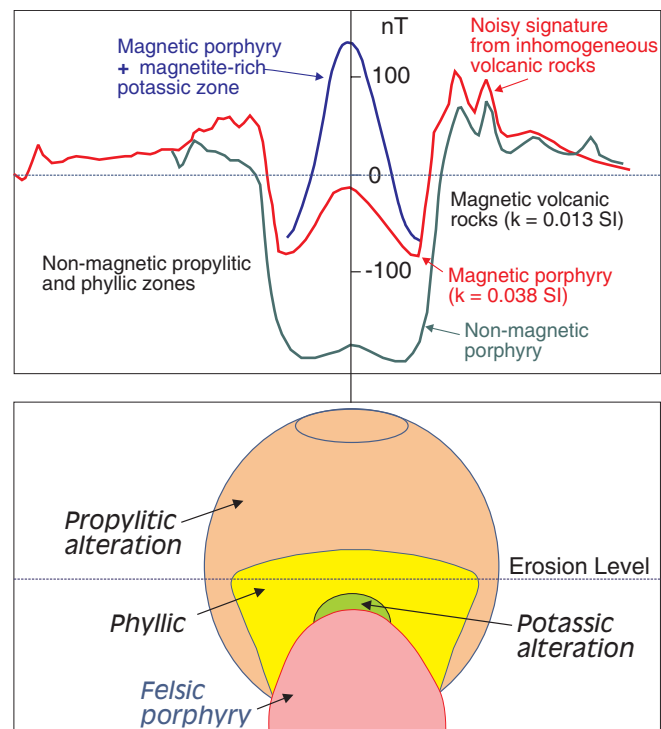


FIGURE 24. Magnetic signatures (assuming a vertical inducing field) associated with an idealized porphyry copper system based on figures in Clark et al. (1992) and Gunn and Dentith (1997).

overlap with the inner potassic and outer propylitic alteration zones. Minerals relevant to geophysical detection include magnetite, pyrite, chalcopyrite, biotite, K-feldspar, and sericite.

Broad, regional aeromagnetic anomalies commonly occur with genetically associated intrusive rocks, and provide a regional exploration target. Mineralization can be associated with magnetite-bearing rocks that would be delineated in an

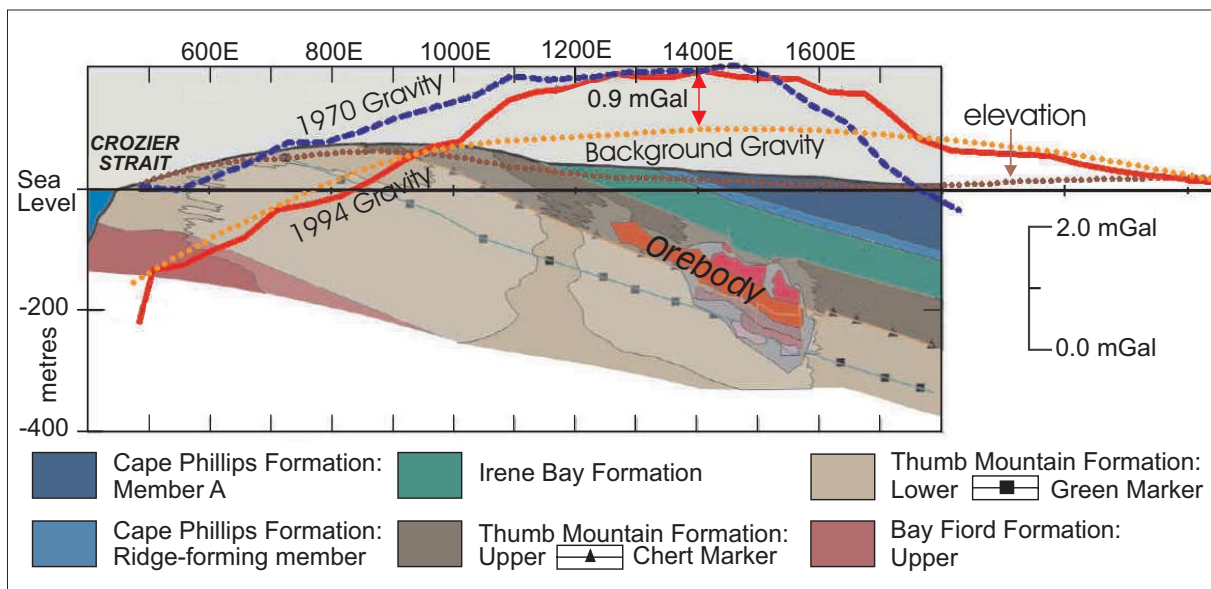


FIGURE 23. Gravity profiles along Line 2200N crossing the Polaris lead-zinc deposit (modified from figure provided by Bob Holroyd, Teck Cominco Ltd.). The density used in the Bouguer correction is 2.67 g/cm^3 .

aeromagnetic survey. Sillitoe (1979) described Au-rich porphyry Cu deposits from several localities worldwide, including examples from the intermontane zone of British Columbia, and noted that the Au is normally found in K-silicate alteration, which is associated with “an unusually high magnetite content”, between 5 to 10% by volume. Mineralization, in some cases, is described as being associated with alteration/magnetite-rich zones on the order of 100s of metres in lateral extent; such zones would present compact and well defined magnetic targets. Hydrothermal alteration may destroy magnetite and may be manifested as a broad, smooth magnetic low. Gunn and Dentith (1997) note that such lows may be associated with zones of propylitic and phyllitic alteration within volcanic rocks capping porphyry intrusions. The volcanic rocks themselves, which are generally inhomogeneous, may produce erratic magnetic responses. Magnetic responses for an idealized porphyry Cu deposit, taken from Gunn and Dentith (1997) and based on Clark et al. (1992), are shown in Figure 24.

Generally K and Th concentrations vary coincidentally with protolith compositions, commonly increasing from mafic to felsic. Subsequent hydrothermal alteration associated with porphyry Cu deposits may disproportionately enrich K such that the ratio $e\text{Th}/K$ produces a diagnostic low value. Airborne gamma-ray spectrometry surveys will map high K anomalies associated with hydrothermal alteration, but these anomalies may be difficult to distinguish from K anomalies associated with normal high-K rock-types. Low $e\text{Th}/K$ ratio anomalies will distinguish K enrichment associated with biotite and K-feldspar alteration from that due to high-K lithologies (Shives et al., 1997). Induced polarization (IP) surveys will delineate pyritic alteration haloes that envelope cupriferous ore zones.

An example of aeromagnetic and airborne gamma-ray spectrometry signatures associated with a porphyry Cu deposit in the Canadian Cordillera is shown in Figure 25. The maps are compiled from airborne data collected along flight lines spaced 500 m apart (Geological Survey of Canada, 1991). At Mount Milligan, a broad magnetic high is associated with exposed and buried portions of the Mount Milligan Intrusive Complex (Fig. 25). High K concentrations are associated with bedrock exposures of the complex

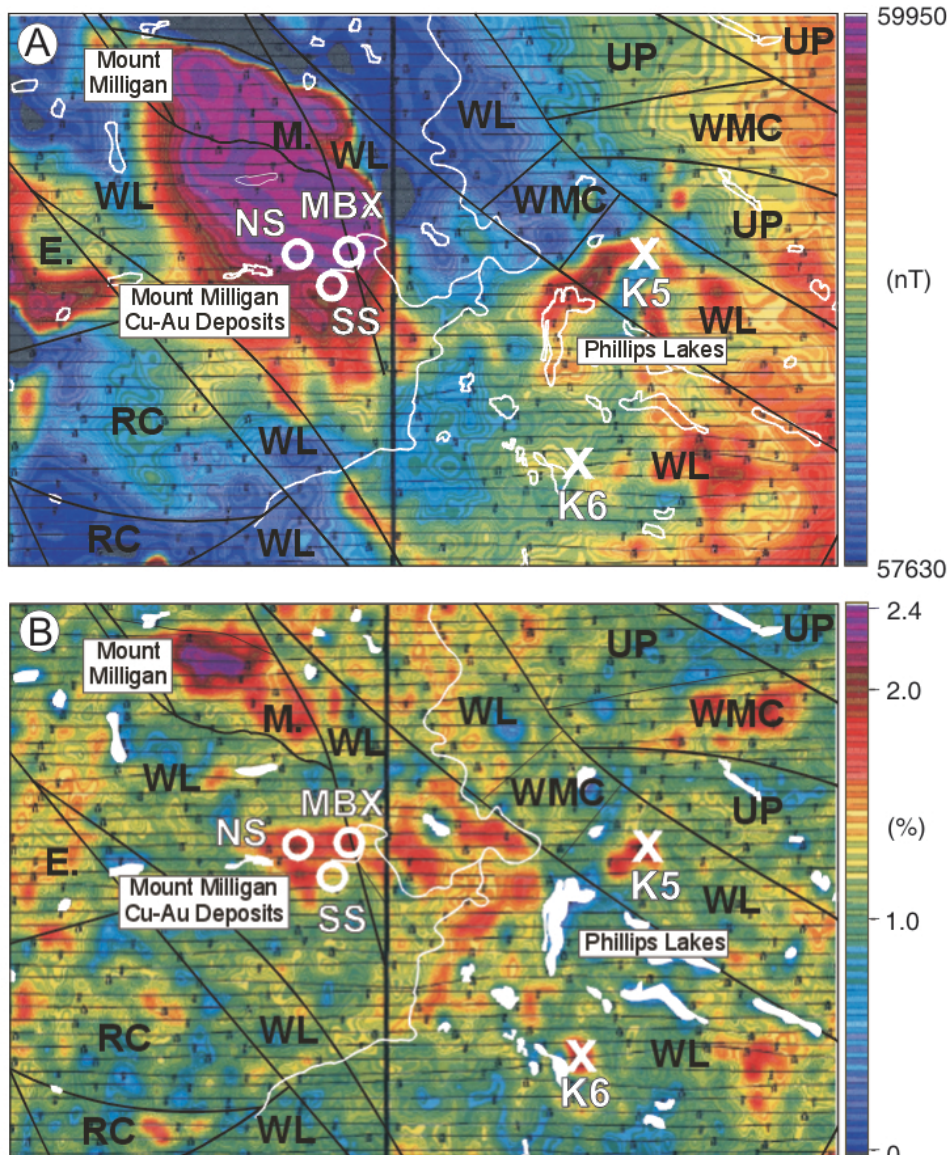


FIGURE 25. (A) Magnetic total field (nT) and (B) potassium (%) signatures in the area of the Mount Milligan porphyry copper deposits (MBX, NS, and SS), British Columbia. E - volcanic wacke; M - Mount Milligan Intrusive Complex, monzonite suite; RC - Rainbow Creek Formation; UP - Mesozoic sedimentary rocks; WL - Witch Lake Formation (Takla Group); WMC - Wolverine Metamorphic Complex.

at Mount Milligan. To the south, discrete K anomalies are associated with the three main zones of the Mount Milligan deposit (MBX, NS, and SS) and provide better defined exploration targets relative to the regional magnetic signatures (Shives et al., 1997). Elsewhere in the survey area, despite extensive and thick overburden, other K anomalies (K5 and K6) are associated, respectively, with K-altered and mineralized andesitic volcanics (K5) and K-altered and mineralized intrusive boulders derived from an unexposed mineralized intrusive unit.

Unconformity-Related Uranium Deposits

Unconformity-related uranium deposits are the most significant high-grade, low-cost source of uranium in the world (Jefferson et al., 2007). In Canada, notable targets for exploration are the mid-Proterozoic sedimentary Athabasca and Thelon basins in the northwestern Canadian Shield. The

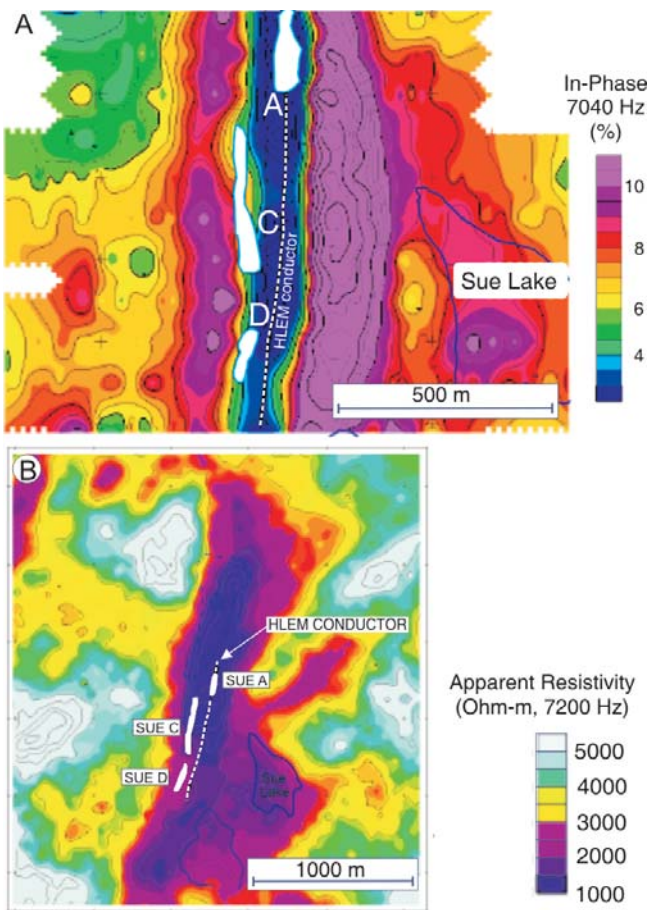


FIGURE 26. Electromagnetic responses over the Sue A, C, and D uranium deposits, Athabasca Basin. (A) MaxMin 1-10 horizontal loop EM in-phase response; (B) Dighem (Airborne) coplanar frequency domain apparent resistivity. Modified from figures published by Matthews et al. (1997).

deposits occur typically along or near unconformities between metamorphic basement rocks, commonly containing graphitic pelitic units, and overlying undeformed sedimentary successions consisting mainly of quartzose sandstone. Graphitic units provide a lithological control on mineralization (Ruzicka, 1995), acting as a reductant. Ruzicka (1995) recognized polymetallic (U-Ni-Co-As) deposits, occurring at the unconformity, and monometallic (U) varieties, generally positioned below the unconformity and rarely above. Faults and fractures intersecting the unconformity are key structures controlling localization of mineralization. Deposit geometry and orientation are characteristically controlled by these structures and the unconformity. Polymetallic orebodies are pod- or lense-shaped and aligned along the structure, whereas monometallic deposits occur as lenses in veins or thin veinlets in stockworks.

Apart from obvious radioactive properties and a high density (up to 9.7 g/cm³), uraninite has no other physical property permitting direct detection by a geophysical technique. Airborne radiometric sur-

veys conducted in 1967 provided the first clues to potential locations of mineralized targets in the Athabasca Basin, outlining many prospective anomalies (Schiller, 1979). Radioactive boulder trains were also of importance in many early discoveries in the Athabasca Basin (Matthews et al., 1997). Drilling of a radioactivity anomaly in an area containing many radioactive boulders in 1968 led to discovery of the Rabbit Lake deposit (Schiller, 1979). Airborne radiometric surveys combined with radioactive boulder studies laid the groundwork for the discovery of the Midwest deposit in 1979 (Scott, 1983). Ground gamma-ray spectrometry measurements also have a role in uranium exploration. For example, Shives et al. (2000) used them to map illitic alteration in sandstones of the Athabasca Basin.

The gravity method is a potential exploration tool where deposits are shallow, but is ineffective in deeper parts of the basin where deposits may be several hundreds of metres deep. Geophysical exploration is, therefore, essentially indirect and focussed on associated structures, alteration, and rock types. Recognition of the relationship between basement graphitic metapelites (conductive), steep faults, and mineralization has resulted in electromagnetic (EM) techniques, both airborne and ground, being the principal exploration methods that narrow the search for prospective zones. Examples of electromagnetic signatures over the cluster of Sue deposits are shown in Figure 26. A MaxMin horizontal loop electromagnetic (HLEM) in-phase response characterized by a linear north-south trending low flanked by two positive shoulders defines the position of a graphitic conductor associated with the deposits (Fig. 26A) (Matthews et al., 1997). This conductor coincides approximately with the axis of a parallel, coincident, linear, apparent resistivity low outlined by an airborne frequency domain survey (coplanar coil configuration) (Fig. 26B).

Electrical techniques, such as IP/resistivity surveys, have been successful in mapping alteration related to mineralization (McMullan et al., 1987; Matthews et al., 1997). At the Cigar Lake deposit, for example, results of time-domain EM surveys failed to record signatures that could be unequivocally tied to the alteration envelope surrounding the deposit, or to the clay-rich paleoregolith at the top of the basement, but resistivity techniques have been successful in mapping alteration (McMullan et al., 1987). An apparent resistivity section crossing the Cigar Lake deposit displays a triangular zone of relatively low apparent resistivities directly above the main pod of the deposit (Fig. 27). This indicates that mineralization-related hydrothermal alteration extends upwards

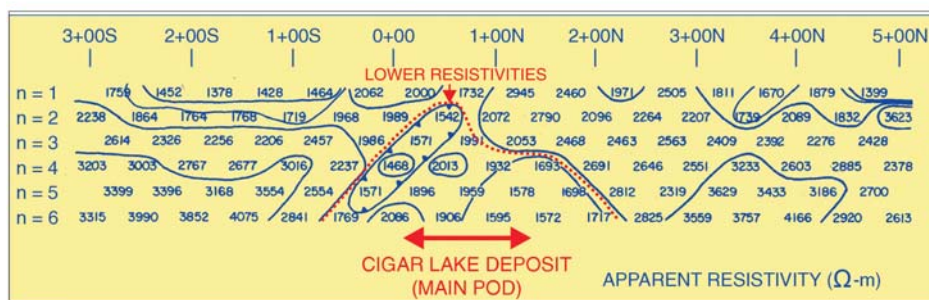


FIGURE 27. An apparent resistivity section crossing the Cigar Lake deposit, Athabasca Basin (after McMullan et al., 1987).

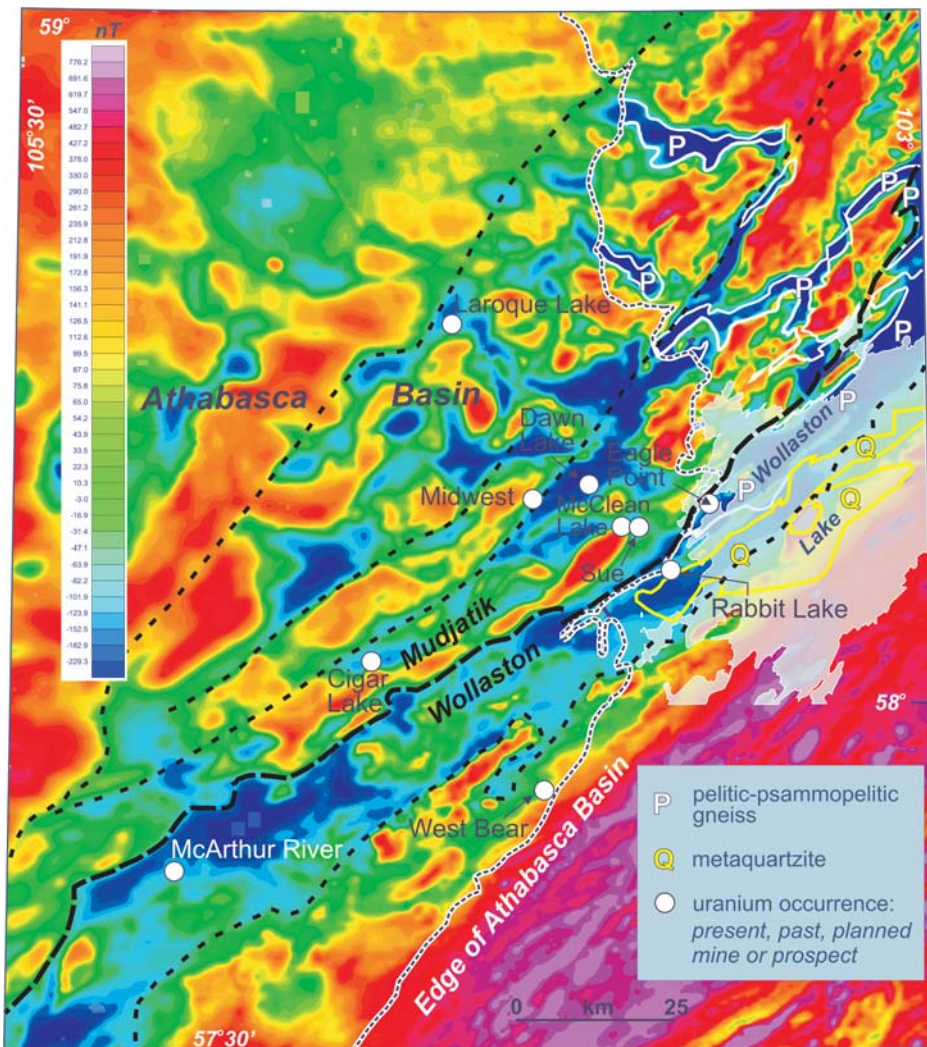


FIGURE 28. Aeromagnetic map (805 m line-spacing; 305 m flight-elevation) of the southeastern margin of the Athabasca Basin and adjacent Wollaston and Mudjatik domains of the Hearne structural province, Canadian Shield. Areas of low magnetic field (blue shades) outside the basin coincide with units of pelitic-psammopelitic gneiss and metaquartzite. Areas of low magnetic field within the basin are considered to signify the presence of similar units below the basin unconformity. These are desired targets for uranium exploration, as substantiated by the discovery of several deposits within or on the flanks of magnetic lows. Figure is based on a figure presented by Thomas and McHardy (in press).

into the Athabasca Basin for more than 400 m (McMullan et al., 1987). On a broader scale, aeromagnetic surveys have been used to map basement lithologies, effectively delineating pelitic metasedimentary rocks containing graphitic units associated with mineralization. These metasedimentary rocks coincide with magnetic lows (Fig. 28). Gravity surveys have been used to map and model faults and palaeotopographic highs on the basement, and to detect and delineate alteration halos characterized by silification (increased density) or desilification (decreased density), both within the basement and overlying sandstone sequences. An example of a negative gravity anomaly (~1 mGal amplitude) associated with an alteration zone within crystalline basement is observed on the southwest grid of the Kiggavik deposit near the margin of the Thelon Basin (Fig. 29). It is attributed mainly to quartz dissolution and filling of voids by water (Hasegawa et al., 1990). Seismic reflection surveys provide critical information on the location and geometry of structures, such as the

basement unconformity and faults that offset it (Fig. 30) (White et al., in press). The seismic method has been effective also in outlining zones of silification within basin sandstones, because of increases in seismic velocity related to silification.

Olympic Dam Type Iron Oxide-Copper-Gold Deposits

Iron oxide Cu-Au (IOCG) deposits represent an important source of Fe and are also a significant deposit type for Cu, U, and REE (Corriveau, 2007). While there are no producing mines in Canada, the most prospective targets for exploration are the Proterozoic granitic and gneissic terranes of the Canadian Shield, and parts of the Cordilleran and Appalachian orogens. Significant examples of IOCG-type deposits in Canada include the NICO and Sue Dianne deposits in the southern part of the Great Bear Magmatic Zone. Corriveau (2007) lists a number of other prospective Proterozoic IOCG districts in Canada, including the Paleoproterozoic Central Mineral Belt of Labrador and the Mesoproterozoic Wernecke Breccias in the Yukon Territory.

IOCG deposits exhibit a wide range of sulphide-deficient, low Ti, magnetite, and/or hematite ore bodies of hydrothermal origin, often genetically associated with granitic to dioritic plutons with A-type geochemical affinities. They display a range of metal contents from

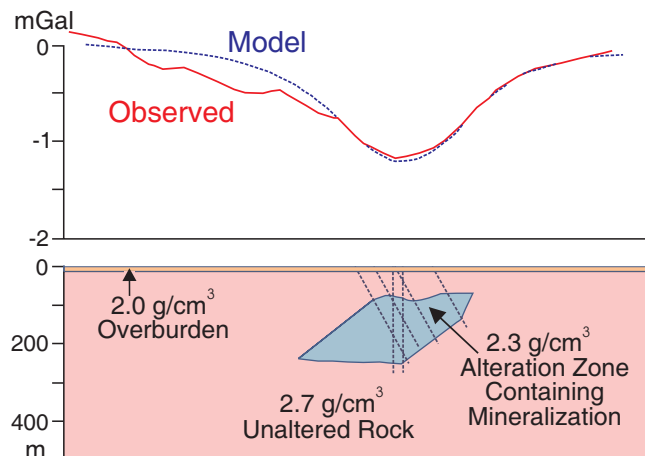


FIGURE 29. Gravity low related to uranium mineralization and alteration zone associated with the Kiggavik deposit (SW grid) within crystalline basement near the margin of the Thelon Basin (after Hasegawa et al., 1990).

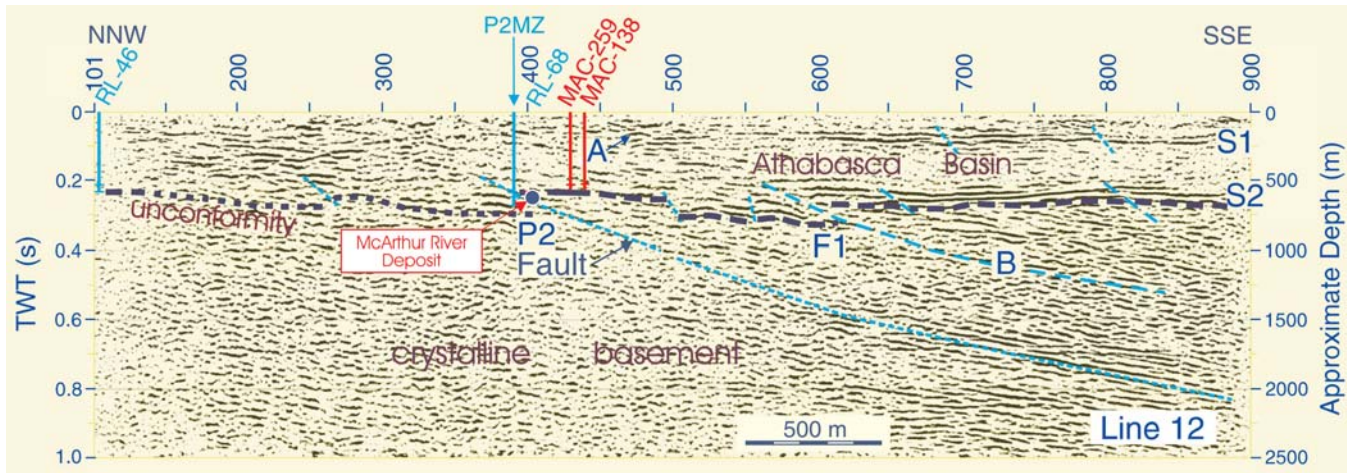


FIGURE 30. Reflection seismic section crossing the McArthur River uranium deposit, Athabasca Basin (modified from figure provided by D.J. White).

monometallic, Kiruna type ($\text{Fe} \pm \text{P}$) to polymetallic Olympic Dam type ($\text{Fe} \pm \text{Cu} \pm \text{U} \pm \text{Au} \pm \text{REE}$) (Lefebvre, 1995; Corriveau, 2007). These deposits occur typically as tabular and pipe-like breccia bodies, veins, and stratiform or discordant disseminations and massive lenses. Because these deposits occur in a wide variety of geological terranes, their host lithologies tend not to be diagnostic. However, the alteration assemblages can be diagnostic with a proximal potassio (sericite and K-feldspar) and Fe-oxide alteration superimposed on a generally more extensive calcic and sodic alteration. Minerals relevant to geophysical detection include Fe-oxide (hematite, martite, magnetite (low-Ti), specularite), Cu sulphides (chalcopyrite, bornite, chalcocite), uraninite, coffinite, sericite, and K-feldspar.

Smith (2002) presented a useful summary of geophysical signatures associated with iron oxide-Cu-Au deposits, and noted that the primary mineralogical characteristic is the abundance of magmatic Fe-oxide and the common relative lack of Fe sulphides. The abundance of mono- and polyphase iron oxide mineralization leads to significant regional and localized aeromagnetic anomalies. Potassio alteration often accompanies the introduction of Cu and Au, and U may also be present. Areas of K alteration may be broad and regionally extensive providing a large exploration target that will produce prominent airborne gamma-ray spectrometry anomalies. The strong magnetic and gamma-ray spectrometry signatures commonly associated with these deposits make combined airborne magnetic and gamma-ray spectrometry surveys an effective exploration tool. High eU and eU/eTh ratio anomalies directly measure U enrichment associated with mineralization, and high K and low eTh/K ratio anomalies are associated with sericitic and/or K-feldspar alteration that can be aerially extensive.

Geophysical signatures of the deposits themselves are however more complex. Whereas deposits are typically located in areas of significant magnetic relief, they do not always coincide with discrete magnetic anomalies. For example, a prominent magnetic anomaly coinciding with the Australian hematite-associated Olympic Dam deposit is apparently related to a deeper source (Smith, 2002). In the case of another Australian deposit, Ernest Henry, an apparently related magnetic response is similar to many other

responses in the area that have no economic significance. This is a common characteristic because related Fe-oxide is generally more widely distributed than Cu and Au mineralization.

Smith (2002) reported that almost all known IOCG deposits produce a significant gravity response, observing that the Olympic Dam deposit produced a significant gravity signature; Ernest Henry also generated a distinct anomaly. Hematite associated with this type of deposit contributes to the gravity signature. As a result of the extensive nature of the disseminated mineralization and the electrical conductivity of breccia cores at some deposits, induced polarization and electromagnetic surveys may be locally applicable, and would complement regional magnetic and gamma-ray spectrometry surveys. Induced polarization and resistivity surveys have been widely used with notable success but will also respond to Fe-oxides and barren sulphides; electromagnetic and magnetotelluric methods have met with success in some cases (Smith, 2002).

A series of gamma-ray spectrometry images and a total magnetic field image compiled from data acquired in an airborne geophysical survey of the Mazenod Lake area, N.W.T., flown along lines spaced 500 m apart is illustrated in Figure 31 (Hetu et al., 1994). These images represent a subset of a larger dataset centred on polymetallic mineralization associated with a broad K anomaly that is coincident with a positive magnetic total field anomaly. At a regional scale, the low eTh/K ratio values distinguish the high K anomalies related to hydrothermal alteration from those associated with normal lithological variations. A gravity anomaly, amplitude 3 mGal, is coincident with the K and magnetic anomalies, and resistivity lows outline mineralized zones (Shives, et al., 1997). A geological cross-section with corresponding pseudo-magnetic and K profiles (from Gandhi et al., 1996) along line AB traversing the Mazenod Lake area Olympic Dam-type mineralization zone is displayed in Figure 32. Both K and magnetic field values are significantly enhanced over the zone.

Magmatic Nickel-Copper-Platinum Group Element Deposits

Eckstrand and Hulbert (2007) define magmatic nickel-copper-PGE deposits as a group of deposits with Ni, Cu, and platinum group elements (PGE) occurring as sulphides in a

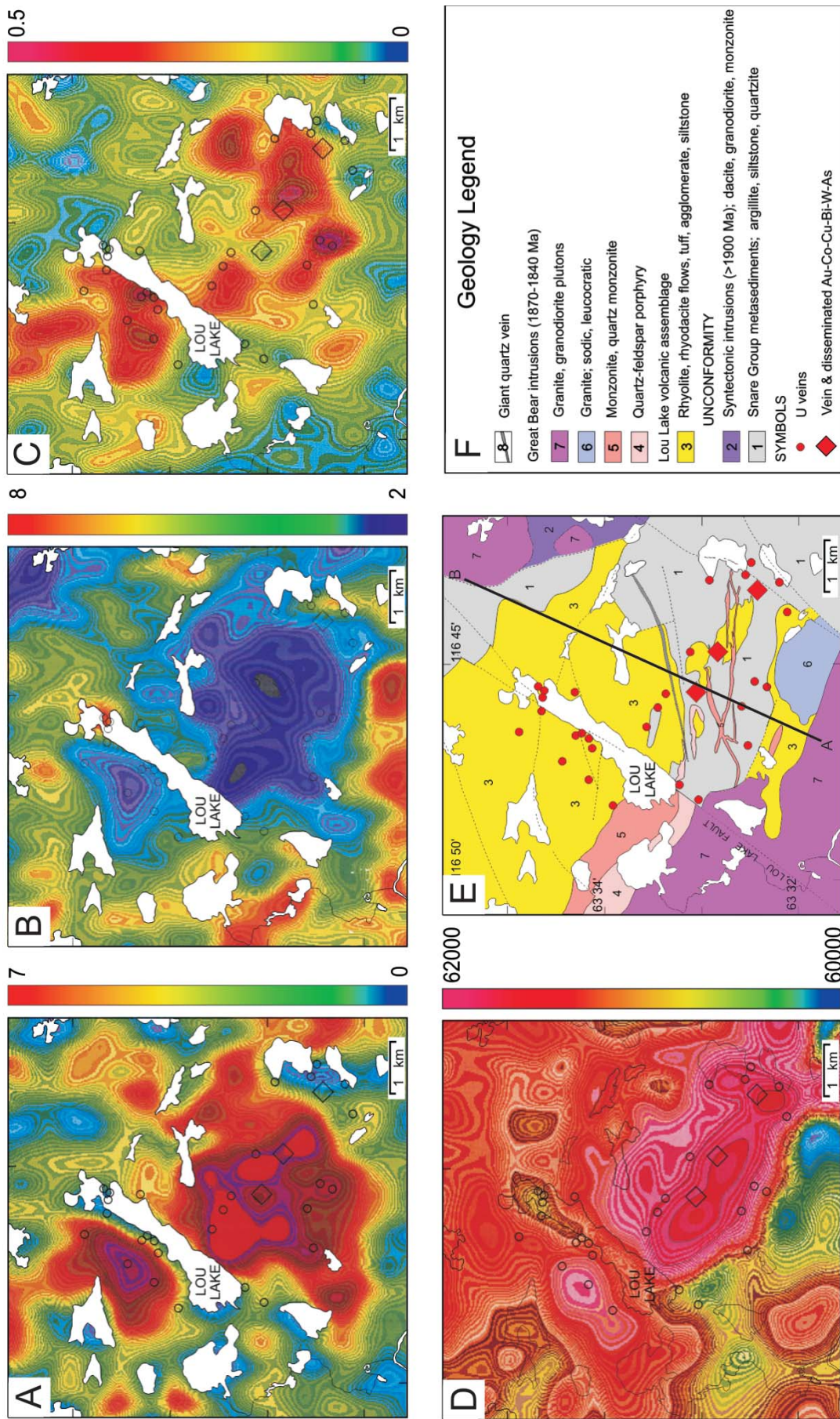


FIGURE 31. Potassium (A), $e\text{Thorium}/e\text{Potassium}$ (B), $e\text{Uranium}/e\text{Thorium}$ (C); and Total magnetic field (D) images for an area near Mazenod Lake, Northwest Territories (Hetu et al., 1994). A geology map (E) and legend (F) (from Gandhi et al., 1996) are also illustrated.

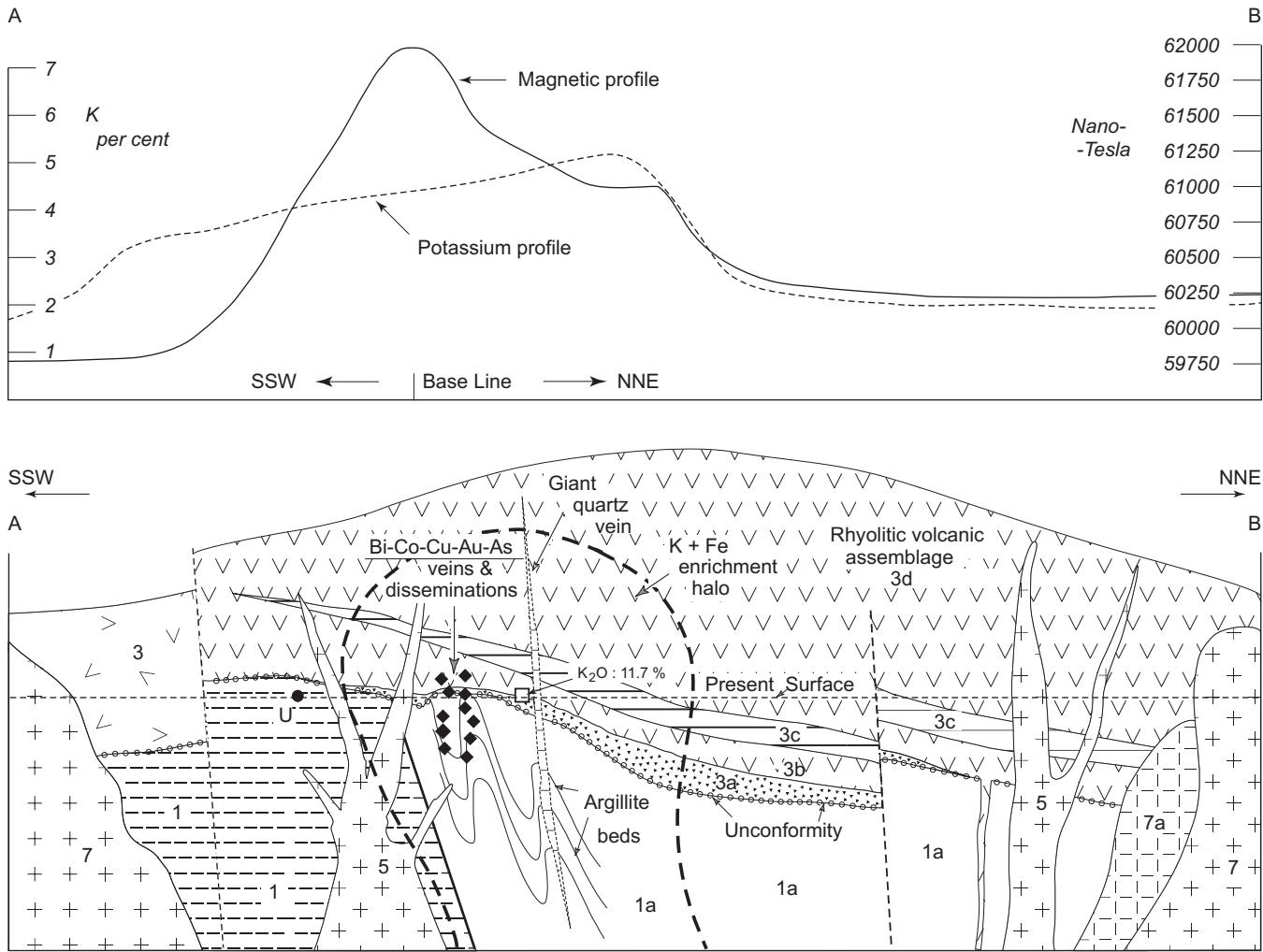


FIGURE 32. Total magnetic field and potassium profiles crossing the mineralized zone in the Mazenod Lake area, Northwest Territories. Legend for the geological cross-section: Unit 1a, quartzite, metasiltstone; Units 3a-3d, rhyolite and ryodacite flows, ignimbrites, volcaniclastic rocks, and undivided rhyolitic rocks; Unit 5, monzonite and quartz monzonite; Unit 7a, dacite, subvolcanic porphyry (from Gandhi et al., 1996).

variety of mafic and ultramafic rocks. These deposits can be divided into two main types. The first type includes Ni-Cu deposits in which sulphide-rich ores are associated with differentiated mafic and/or ultramafic flows and sills. The second type is represented by deposits mined primarily for PGE's that are associated with sparsely dispersed sulphides in mafic/ultramafic layered intrusions.

In Ni-Cu deposits, Ni is usually the main economic commodity with Cu a co-product or by-product along with Co, PGE, and Au. The host rocks for these deposits include meteorite-impact mafic melts (Sudbury, Ontario), rift and continental flood basalt-associated mafic sills and dyke-like bodies (Noril'sk-Talnakh, Russia), komatiitic (magnesium-rich) volcanic flows and related sill-like intrusions (Thompson, Manitoba), and other mafic/ultramafic intrusions such as Voisey's Bay, Labrador (Eckstrand and Hulbert, 2007). PGE deposits can be divided into two main subtypes. These include reef-type or stratiform deposits hosted by well layered mafic/ultramafic intrusions (Merensky Reef, Bushveld Complex, South Africa) and magmatic breccia-type deposits hosted by stock-like or layered mafic/ultramafic intrusions (Lac des Iles, Ontario).

Both Ni-Cu-PGE and PGE deposits are associated with large mafic/ultramafic igneous complexes that can easily be detected, at a regional scale, by magnetic and gravity methods. This is the case, for example, for the Muskox, Thompson, and Raglan orebodies. Magnetics is therefore the main geophysical technique to map host rocks for this deposit type. The presence of pyrrhotite in the deposit may create a magnetic anomaly, although it can be lost in the strong magnetic anomalies of the associated intrusive rocks. In addition, gravity can be used to identify deposits at the detailed exploration scale because they have a high-density contrast with their host rocks.

The Ni-Cu-PGE sulphide deposits consist of highly conductive sulphides (pyrrhotite, pentlandite, and chalcopyrite) that produce large frequency domain EM anomalies. They sometimes can be difficult to detect with time-domain EM systems as their response is at the upper limit of the aperture of these systems, although they are identifiable from their slow decay. In the case of low-sulphide PGE deposits, high-resolution frequency-domain EM data are effective in identifying this type of mineralization, although they may generate only weak EM anomalies. However, high-resolution fre-

Overview of Geophysical Signatures Associated with Canadian Ore Deposits

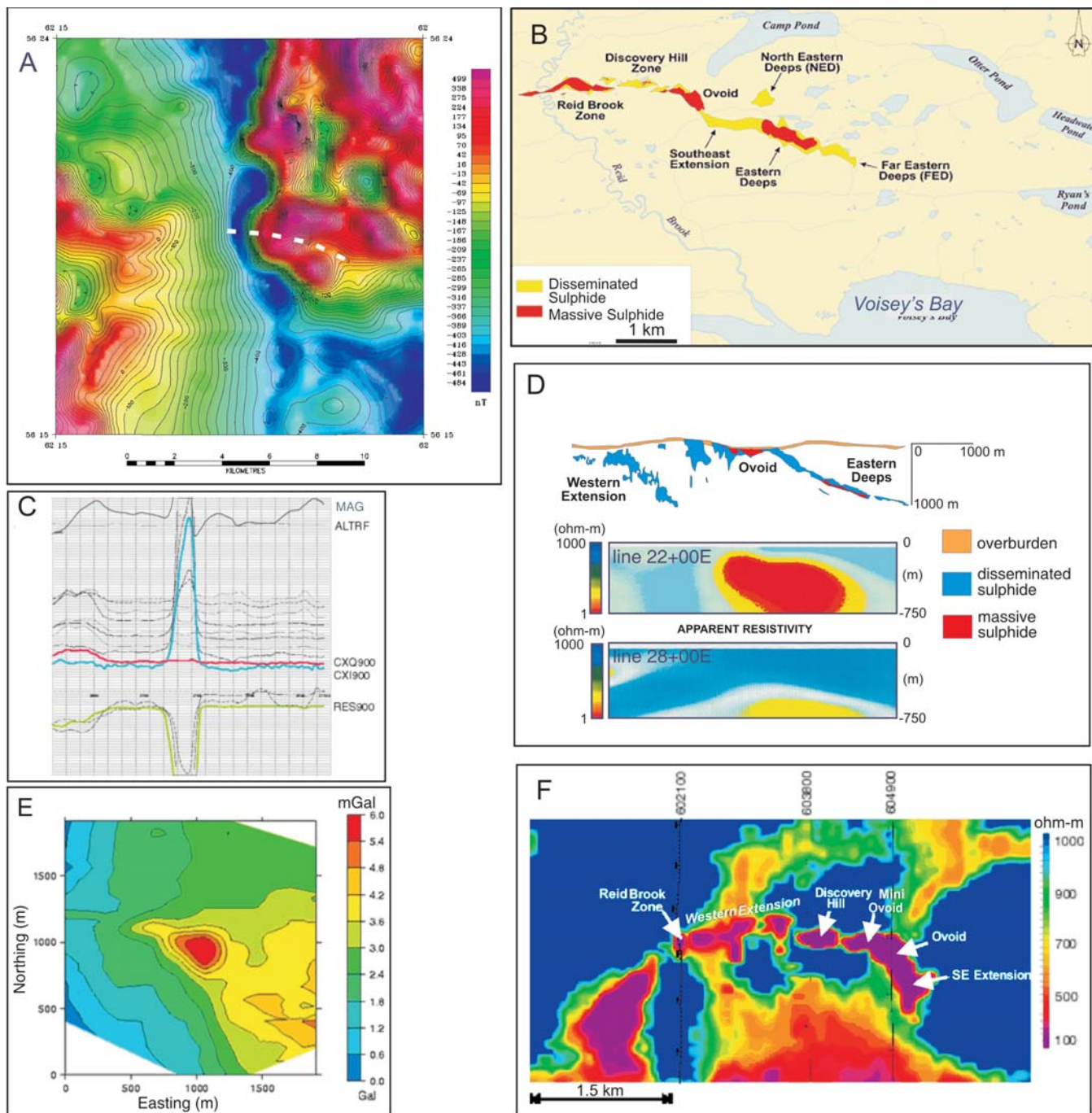


FIGURE 33. Geophysical signatures over nickel-copper-PGE orebodies, Voisey's Bay, Labrador. **(A)** Total magnetic field (white dashed line traces location of sulphide deposits); **(B)** Location and extent of the Voisey's Bay sulphide deposits (image from: www.gov.nf.ca); **(C)** strong EM response detected by a helicopter survey over the Ovoid Zone (image from: www.fugroairborne.com); **(D)** apparent resistivities calculated from an audio magnetotelluric survey over the Eastern Deeps massive sulphide body (after Balch, 1999); **(E)** Bouguer gravity anomaly, of approximately 4 mGal amplitude, over the Ovoid Zone (image from: <http://www.geop.ubc.ca/ubcgif>); **(F)** apparent resistivity at 900 Hz as defined by a Dighem HEM survey; the Voisey's Bay sulphide bodies are clearly outlined by an area of low resistivity (image from: www.fugroairborne.com).

quency-domain EM data can be corrected for the magnetic susceptibility of the mineralization and the host rocks and help highlight the response of low-sulphide PGE deposits (Huang and Fraser, 2000).

At the Voisey's Bay deposit, strong frequency-domain EM anomalies are observed over the Ovoid zone (Fig. 33). The apparent width of the deposit is 500 m, and the conductance is thousands of Siemens. Apparent resistivity is less

than that of seawater. A small magnetic anomaly (not visible in the regional data shown above) is measured over the deposit. As a whole, there is no strong correlation between the total magnetic field and the known mineralization (Balch, 1999).

TABLE 4. Utility of geophysical methods in exploration for specific mineral deposit types.

Geophysical Method	Air or Ground	Application	Diamonds	Lode Gold	VMS Deposits	MVT Lead-Zinc Deposits	SEDEX Deposits	Porphyry Copper Deposits	Uranium Deposits	Olympic Dam-Type Deposits	Magmatic Ni-Cu-PGEs Deposits
MAGNETIC	Air	Geological Framework	●	●	●	●	●	●	●	●	●
		Direct Targeting	●	●	●	●	●	●	●	●	●
	Ground	Geological Framework	●	●	●	●	●	●	●	●	●
		Direct Targeting	●	●	●	●	●	●	●	●	●
ELECTRO-MAGNETIC	Air	Geological Framework	●	●	●	●	●	●	●	●	●
		Direct Targeting	●	●	●	●	●	●	●	●	●
	Ground	Geological Framework	●	●	●	●	●	●	●	●	●
		Direct Targeting	●	●	●	●	●	●	●	●	●
ELECTRIC	Ground	Geological Framework	●	●	●	●	●	●	●	●	●
		Direct Targeting	●	●	●	●	●	●	●	●	●
GRAVITY	Air	Geological Framework	●	●	●	●	●	●	●	●	●
		Direct Targeting	●	●	●	●	●	●	●	●	●
	Ground	Geological Framework	●	●	●	●	●	●	●	●	●
		Direct Targeting	●	●	●	●	●	●	●	●	●
RADIOMETRIC	Air	Geological Framework	●	●	●	●	●	●	●	●	●
		Direct Targeting	●	●	●	●	●	●	●	●	●
	Ground	Geological Framework	●	●	●	●	●	●	●	●	●
		Direct Targeting	●	●	●	●	●	●	●	●	●
SEISMIC	Ground	Geological Framework	●	●	●	●	●	●	●	●	●
		Direct Targeting	●	●	●	●	●	●	●	●	●

Qualitative Applicability Rating of Geophysical Method: ● Highly Effective ● Moderately Effective ● Generally Ineffective

Conclusions

Geophysical techniques have made, and continue to make, a major contribution to exploration for a variety of mineral deposit types. This report provides a short overview of the more commonly used methods and illustrates the types of signatures that may be expected over specific deposit types. The suites of signatures are by no means comprehensive, and signatures may differ to varying degrees depending on local geology and mineralogy.

A qualitative assessment of the utility of the different geophysical techniques in the exploration for the different deposit types is attempted in Table 4 with respect to 1) direct detection and (2) framework mapping. In this table, direct detection also covers targets that are somewhat larger than the sought after orebody, such as a potassic alteration halo outlined by a radiometric survey. Framework mapping covers the aspect of geophysical mapping of lithology and structure, usually at a regional or semi-regional scale, but also including property-scale mapping. It is cautioned that Table 4 represents a qualitative evaluation of the efficacy of the techniques. As such it is rather generalized and it is acknowledged that examples may exist that might not be consistent with the ranking of a technique as presented.

Published documentation of geophysical attributes of Canadian ore deposits is limited and hence potentially valuable case histories that could benefit the explorationist are unavailable. In spite of this shortcoming, the existing docu-

mentation, together with numerous company web sites displaying geophysical images of properties and mineralization in various stages of exploration and evaluation, provide a reasonably complete spectrum of geophysical responses for several deposit types. Furthermore, the mineralogical and related rock property data for all types of ore deposits are sufficiently well known that a selection of suitable geophysical techniques can be readily made.

Even relatively new geophysical techniques, such as airborne scalar and full tensor gravimetry, deep EM methods that can investigate at depths of 1 or 2 km, tensor magnetics, etc., rely on the detection of physical property contrasts. The joint use of modern 3-D geophysical inversion, used to build physical property models, and 3-D geological models will certainly be essential for the discovery of future mineral deposits.

Acknowledgements

We thank Bob Holroyd and Boris Lum (Teck Cominco Limited) for the image of gravity profiles crossing the Polaris deposit, Nunavut, Sue Davis and Rob Shives (Geological Survey of Canada), respectively, for drafting services and discussions relating to gamma-ray spectrometry data, Wayne Goodfellow (Geological Survey of Canada) for editorial comment, and Bill Morris (McMaster University) for refereeing the manuscript.

References

- Ash, C., and Alldrick, D., 1996, Au-quartz veins, in Lefebvre, D.V., and Höy, T., eds., Selected British Columbia Mineral Deposit Profiles, Volume 2 – Metallic Deposits: British Columbia Ministry of Employment and Investment, Open File 1996-13, p. 53-56.
- Balch, S.E., 1999, Ni-Cu sulphide deposits with examples from Voisey's Bay, in Lowe, C., Thomas, M.D., and Morris, W.A., eds., Geophysics in Mineral Exploration: Fundamentals and Case Histories: Geological Association of Canada, Short Course Notes, v. 14, p. 21-40.
- Belland, M., 1992, The Birth of the Bathurst Mining Camp: A Development History of the Austin Brook Iron Mine and No. 6 Base-Metal Deposit: New Brunswick Department of Natural Resources and Energy, Popular Geology Paper 92-1, 56 p.
- Bishop, J.R., and Emerson, D.W., 1999, Geophysical properties of zinc-bearing minerals: Australian Journal of Earth Sciences, v. 46, p. 311-328.
- Brock, J.S., 1973, Geophysical exploration leading to the discovery of the Faro deposit: Canadian Mining and Metallurgical Bulletin, v. 66, p. 97-116.
- Broome, J., Carson, J.M., Grant, J.A., and Ford, K.L., 1987, A Modified Ternary Radiolelement Mapping Technique and Its Application to the South Coast of Newfoundland: Geological Survey of Canada, Paper 87-14, scale 1:500 000.
- Brownell, G.M., 1950, Radiation surveys with a scintillation counter: Economic Geology, v. 45, p. 167-174.
- Brummer, J.J., MacFadyen, D.A., and Pegg, C.C., 1992, Discovery of kimberlites in the Kirkland Lake area, Northern Ontario, Canada; Part II: Kimberlite discoveries, sampling, diamond content, ages and emplacement: Exploration Mining Geology, v. 1, p. 351-370.
- Carmichael, R.S., 1982, Practical Handbook of Physical Properties of Rocks, Volume II: CRC Press, 340 p.
- Clark, D.A., French, D.H., Lackie, M.A., and Schmidt, P.W., 1992, Magnetic petrology: Application of integrated rock magnetic and petrological techniques to geological interpretation of magnetic surveys: Exploration Geophysics, v. 23, p. 65-58.
- Corriveau, L., 2007, Iron oxide copper-gold deposits: A Canadian perspective, in Goodfellow, W.D., ed., Mineral Deposits of Canada: A Synthesis of Major Deposit-Types, District Metallogeny, the Evolution of Geological Provinces, and Exploration Methods: Geological Association of Canada, Mineral Deposits Division, Special Publication No. 5, p. 307-328.
- Dewing, K., Sharp, R.J., and Turner, E., 2007, Synopsis of the Polaris Zn-Pb district, Canadian Arctic Islands, Nunavut, in Goodfellow, W.D., ed., Mineral Deposits of Canada: A Synthesis of Major Deposit-Types, District Metallogeny, the Evolution of Geological Provinces, and Exploration Methods: Geological Association of Canada, Mineral Deposits Division, Special Publication No. 5, p. 655-672.
- Dickson, B.L., and Scott, K.M., 1997, Interpretation of aerial gamma-ray surveys – adding the geochemical factors: AGSO Journal of Australian Geology and Geophysics, v. 17, p. 187-200.
- Dubé, B., and Gosselin, P., 2007, Greenstone-hosted quartz-carbonate vein deposits, in Goodfellow, W.D., ed., Mineral Deposits of Canada: A Synthesis of Major Deposit-Types, District Metallogeny, the Evolution of Geological Provinces, and Exploration Methods: Geological Association of Canada, Mineral Deposits Division, Special Publication No. 5, p. 49-73.
- Dubé, B., Gosselin, P., Hannington, M.D., and Galley, A., 2007, Gold-rich volcanogenic massive sulphide deposits, in Goodfellow, W.D., ed., Mineral Deposits of Canada: A Synthesis of Major Deposit-Types, District Metallogeny, the Evolution of Geological Provinces, and Exploration Methods: Geological Association of Canada, Mineral Deposits Division, Special Publication No. 5, p. 75-94.
- Durocher, M.E., 1983, The nature of hydrothermal alteration associated with the Madsen-Starrett-Olsen deposits, Red lake area, in Colvine, A.C., ed., The Geology of Gold in Ontario: Ontario Geological Survey, Miscellaneous Paper 110, p. 123-140.
- Eckstrand, O.R., and Hulbert, L., 2007, Magmatic nickel-copper-platinum group element deposits, in Goodfellow, W.D., ed., Mineral Deposits of Canada: A Synthesis of Major Deposit-Types, District Metallogeny, the Evolution of Geological Provinces, and Exploration Methods: Geological Association of Canada, Mineral Deposits Division, Special Publication No. 5, p. 205-222.
- Fraser, D.C., 1973, Magnetite ore tonnage estimates from an aerial electromagnetic survey: Geoexploration, v. 11, p. 97-105.
- Galley, A., Hannington, M., and Jonasson, I., 2007, Volcanogenic massive sulphide deposits, in Goodfellow, W.D., ed., Mineral Deposits of Canada: A Synthesis of Major Deposit-Types, District Metallogeny, the Evolution of Geological Provinces, and Exploration Methods: Geological Association of Canada, Mineral Deposits Division, Special Publication No. 5, p. 141-161.
- Gandhi, S.S., Prasad, N., and Charbonneau, B.W., 1996, Geological and geophysical signatures of a large polymetallic exploration target at Lou Lake, southern Great Bear magmatic zone, Northwest Territories: Geological Survey of Canada, Current Research 1996-E, p. 147-158.
- Gendzwill, D.J., and Matieshin, S.D., 1996, Seismic reflection survey of a kimberlite intrusion in the Fort à la Corne district, Saskatchewan, in Lecheminant, A.N., Richardson, D.G., DiLabio, R.N.W., and Richardson, K.A., eds., Searching for Diamonds in Canada: Geological Survey of Canada, Open File 3228, p. 251-253.
- Geological Survey of Canada, 1991, Airborne geophysical survey, Mount Milligan area, British Columbia (NTS 930/4W, N1, N2E): Open File 2535, scale 1:100 000.
- Ghosh, M.K., 1972, Interpretation of airborne EM measurements based on thin sheet models: Research in Applied Geophysics, No. 4, University of Toronto.
- Goodacre, A.K., Brule, B.G., and Cooper, R.V., 1969, Results of regional underwater gravity surveys in the Gulf of St. Lawrence: Department of Energy, Mines and Resources, Gravity Map Series of the Earth Physics Branch, No. 86, Ottawa.
- Goodfellow, W.D., and Lydon, J., 2007, Sedimentary-exhalative (SEDEX) deposits, in Goodfellow, W.D., ed., Mineral Deposits of Canada: A Synthesis of Major Deposit-Types, District Metallogeny, the Evolution of Geological Provinces, and Exploration Methods: Geological Association of Canada, Mineral Deposits Division, Special Publication No. 5, p. 163-183.
- Grant, F.S., and West, G.F., 1965, Interpretation Theory in Applied Geophysics: International Series in the Earth Sciences, McGraw-Hill Book Company, New York, 584 p.
- Grasty, R.L., and Minty, B.R.S., 1995, A Guide to the Technical Specifications for Airborne Gamma-Ray Surveys: Australian Geological Survey Organization, Record 1995/60, 89 p.
- Grasty, R.L., Mellander, H., and Parker, M., 1991, Airborne Gamma-Ray Spectrometer Surveying: International Atomic Energy Agency, Technical Report Series 323, Vienna, 97 p.
- Gunn, P.J., and Dentith, M.C., 1997, Magnetic responses associated with mineral deposits: AGSO Journal of Australian Geology and Geophysics, v. 17, p. 145-158.
- Hannigan, P.K., 2007, Metallogeny of the Pine Point Mississippi Valley-type zinc-lead district, southern Northwest Territories, in Goodfellow, W.D., ed., Mineral Deposits of Canada: A Synthesis of Major Deposit-Types, District Metallogeny, the Evolution of Geological Provinces, and Exploration Methods: Geological Association of Canada, Mineral Deposits Division, Special Publication No. 5, p. 609-632.
- Hasegawa, K., Davidson, G.I., Wollenberg, P., and Iida, Y., 1990, Geophysical exploration for unconformity-related uranium deposits in the northeastern part of the Thelon Basin, Northwest Territories, Canada: Mining Geology, v. 40, p. 83-94.
- Hearst, R.B., Morris, W.A., and Schieck, D.G., 1994, Reflection seismic profiling for massive sulphides in the high Arctic: 64th Annual International Meeting, Society of Exploration Geophysicists, p. 531-533.
- Hetu, R.J., 1991, Airborne Geophysical Survey, Red Lake, Ontario: Geological Survey of Canada, Open File 2403, 41 p.
- Hetu, R.J., Holman, P.B., Charbonneau, B.W., Prasad, N., and Gandhi, S.S., 1994, Multiparameter Airborne Geophysical Survey of the Mazenod Lake Area, Northwest Territories: Geological Survey of Canada, Open File 2806, 100 p.
- Hood, P.J., and Teskey, D.J., 1989, Aeromagnetic gradiometer program of the Geological Survey of Canada: Geophysics, v. 54, p. 1012-1022.
- Hoover, D.B., and Campbell, D.L., 1992, Geophysical models of diamond pipes, Cox and Singer model 12, in Hoover, D.B., Heran, W.D., and Hill, P.L., eds., The Geophysical Expression of Selected Mineral Deposits: United States Department of the Interior, Geological Survey, Open File Report 92-557, p. 85-88.
- Horsfall, K.R., 1997, Airborne magnetic and gamma-ray data acquisition: AGSO Journal of Australian Geology and Geophysics, v. 17, p. 23-30.

- Huang, H., and Fraser, D. C., 2000, Airborne resistivity and susceptibility mapping in magnetically polarizable areas. *Geophysics*, v. 65, p. 502-511.
- Hunt, C.P., Moskowitz, B.M., and Banerjee, S.K., 1995, Magnetic properties of rocks and minerals, in Ahrens, T.J., ed., *Rock Physics and Phase Relations: A Handbook of Physical Constants*: American Geophysical Union Reference Shelf 3, American Geophysical Union, p. 189-204.
- International Atomic Energy Agency, 2003, Guidelines for radioelement mapping using gamma ray spectrometry data. IAEA-TECDOC-1363, 173 p.
- Jefferson, C.W., Thomas, D.J., Gandhi, S.S., Ramaekers, P., Delaney, G., Brisbin, D., Cutts, C., Quirt, D., Portella, P., and Olson, R.A., 2007, Unconformity-associated uranium deposits of the Athabasca Basin, Saskatchewan and Alberta, in Goodfellow, W. D., ed., *Mineral Deposits of Canada: A Synthesis of Major Deposit-types, District Metallogeny, the Evolution of Geological Provinces, and Exploration Methods*, Mineral Deposits Division, Geological Association of Canada, Special Publication 5, p. 273-305.
- Katsube, T.J., and Kjarsgaard, B.A., 1996, Physical characteristics of Canadian kimberlites, in Lecheminant, A.N., Richardson, D.G., DiLabio, R.N.W., and Richardson, K.A., eds., *Searching for Diamonds in Canada: Geological Survey of Canada, Open File 3228*, p. 241-242.
- Keating, P., 1995, A simple technique to identify magnetic anomalies due to kimberlite pipes: *Mining and Exploration Geology*, v. 4, p. 121-125.
- , 1996, Kimberlites and aeromagnetics, in Lecheminant, A.N., Richardson, D.G., DiLabio, R.N.W., and Richardson, K.A., eds., *Searching for Diamonds in Canada: Geological Survey of Canada, Open File 3228*, p. 233-236.
- Keller, G.V., and Frischknecht, F.C., 1966, *Electrical Methods in Geophysical Prospecting: International Series on Monographs on Electromagnetic Waves*, Volume 10: Pergamon Press Inc., 519 p.
- Killeen, P.G., 1979, Gamma-ray spectrometric methods in uranium exploration – application and interpretation, in Hood, P.J., ed., *Geophysics and Geochemistry in Search for Metallic Ores: Geological Survey of Canada, Economic Geology Report 31*, p. 163-230.
- Kjarsgaard, B.A., 1996, Kimberlites, in Lecheminant, A.N., Richardson, D.G., DiLabio R.N.W., and Richardson, K.A., eds., *Searching for Diamonds in Canada: Geological Survey of Canada, Open File 3228*, p. 29-37.
- , 2007, Kimberlite diamond deposits, in Goodfellow, W.D., ed., *Mineral Deposits of Canada: A Synthesis of Major Deposit-types, District Metallogeny, the Evolution of Geological Provinces, and Exploration Methods*: Geological Association of Canada, Mineral Deposits Division, Special Publication No. 5, p. 245-272.
- Klein, C., and Hurlbut, C.S., 1985, *Manual of Mineralogy* (after J.D. Dana), 20th Edition: John Wiley and Sons, New York, 596 p.
- Klein, D.P., and Bankey, V., 1992, Geophysical model of Creede, Comstock, Sado, Goldfield and related epithermal precious metal deposits, in Hoover, D.B., Heran, W.D., and Hill, P.L., eds., *The Geophysical Expression of Selected Mineral Deposits: United States Department of the Interior, Geological Survey, Open File Report 92-557*, p. 98-106.
- Lajoie, J.L., and Klein, J., 1979, Geophysical exploration at the Pine Point Mines Ltd. zinc-lead property, Northwest Territories, Canada, in Hood, P.J., ed., *Geophysics and Geochemistry in the Search for Metallic Ores: Proceedings of Exploration 1977*, Geological Survey of Canada, Economic Geology Report 31, p. 652-664.
- Lane, R.J.L., ed., 2004, Abstract from the ASEG-PESA Airborne Gravity 2004 Workshop: *Geoscience Australia Record 2004/18*, 141 p.
- Lang, A.H., 1953, The development of portable geiger counters: *Canadian Mining Journal*, v. 74, p. 65-68.
- Lecheminant, A.N., and Kjarsgaard, B.A., 1996, Part 1: Geology, petrology, and geotectonic controls – Introduction, in Lecheminant, A.N., Richardson, D.G., DiLabio, R.N.W., and Richardson, K.A., eds., *Searching for Diamonds in Canada: Geological Survey of Canada, Open File 3228*, p. 5-9.
- Lefebure, D.V., 1995, Iron oxide breccias and veins P-Cu-Au-Ag-U, in Lefebure, D.V. and Ray, G.E., eds., *Selected British Columbia Mineral Deposit Profiles, Volume 1 – Metallics and Coal*: British Columbia Ministry of Energy of Employment and Investment, Open File 1995-20, p. 33-36.
- Lehnert-Thiel, K., Loewer, R., Orr, R. G., and Robertshaw, P., 1992, Diamond-bearing kimberlites in Saskatchewan, Canada: The Fort à la Corne case history: *Exploration and Mining Geology*, v. 1, p. 391-403.
- Lowe, C., Brown, D.A., Best, M.E., and Shives, R.B., 2000, High resolution geophysical survey of the Purcell Basin and Sullivan deposit: Implications for bedrock geology and mineral exploration, in Lydon, J.W., Slack, J.F., Höy, T., and Knapp, M.E., eds., *The Geological Environment of the Sullivan Deposit, British Columbia: Geological Association of Canada, Mineral Deposits Division, Special Volume No. 1*, p. 279-293.
- Lydon, J.W., 1984, Volcanogenic massive sulphide deposits, Part 1: A descriptive model: *Geoscience Canada*, v. 11, p. 195-202.
- , 1995, Sedimentary exhalative sulphides (SEDEX), in Eckstrand, O.R., Sinclair, W.D., and Thorpe, R.I., eds., *Geology of Canadian Mineral Deposit Types: Geological Survey of Canada, Geology of Canada, no. 8*, p. 130-152 (also Geological Society of America, *Geology of North America*, v. P-1).
- Lydon, J.W., Goodfellow, W.D., Dubé, B., Paradis, S., Sinclair, W.D., Corriveau, L., and Gosselin, P., 2004, A Preliminary Overview of Canada's Mineral Resources: Geological Survey of Canada, Open File 4668, 20 p.
- Macnae, J.C., 1979, Kimberlites and exploration geophysics: *Geophysics*, v. 44, p. 1395-1416.
- Macnae, J., 1995, Applications of geophysics for the detection and exploitation of kimberlites and lamproites, in Griffin, W.L., ed., *Diamond Exploration into the 21st Century: Journal of Geochemical Exploration*, v. 53, p. 213-243.
- Matthews, R., Koch, R., and Leppin, M., 1997, Paper 130: Advances in integrated exploration for unconformity uranium deposits in Western Canada, in Gubins, A.G., ed., *Proceedings of Exploration 97: Fourth Decennial International Conference on Mineral Exploration: Geophysics and Geochemistry at the Millennium*: p. 993-1024 (CD-ROM).
- McMullan, S.R., Matthews, R.B., and Robertshaw, P., 1987, Exploration geophysics for Athabasca uranium deposits, in Garland, G.D., ed., *Proceedings of Exploration '87: Third Decennial International Conference on Geophysical and Geochemical Exploration for Minerals and Groundwater: Ontario Geological Survey, Special Volume 3*, p. 547-566.
- Minty, B.R.S., 1997, Fundamentals of airborne gamma-ray spectrometry: *AGSO Journal of Australian Geology and Geophysics*, v. 17, p. 39-50.
- Minty, B.R.S., Luyendyk, A.P.J., and Brodie, R.C., 1997, Calibration and data processing for airborne gamma-ray spectrometry: *AGSO Journal of Australian Geology and Geophysics*, v. 17, p. 51-62.
- Mitchell, R.H., 1986, *Kimberlites: Mineralogy, Geochemistry, and Petrography*: Plenum Press, New York, 442 p.
- Mwenifumbo, C.J., and Kjarsgaard, B., 2002, Kimberlite investigations using borehole geophysics: Abstracts of Saskatoon 2002 Geological Association of Canada-Mineralogical Association of Canada Convention.
- Palacky, G., 1986, *Airborne Resistivity Mapping: Geological Survey of Canada, Paper 86-2*, 195 p.
- Panteleyev, A., 1996a, Epithermal Au-Ag: Low Sulphidation, in Lefebure, D.V., and Höy, T., eds., *Selected British Columbia Mineral Deposit Profiles, Volume 2 – Metallic Deposits: British Columbia Ministry of Employment and Investment, Open File 1996-13*, p. 41-44.
- , 1996b, Epithermal Au-Ag-Cu: High Sulphidation, in Lefebure, D.V., and Höy, T., eds., *Selected British Columbia Mineral Deposit Profiles, Volume 2 – Metallic Deposits: British Columbia Ministry of Employment and Investment, Open File 1996-13*, p. 37-39.
- Paradis, S., and Nelson, J.L., 2007, Metallogeny of the Robb Lake carbonate-hosted zinc-lead district, northeastern British Columbia, in Goodfellow, W.D., ed., *Mineral Deposits of Canada: A Synthesis of Major Deposit-types, District Metallogeny, the Evolution of Geological Provinces, and Exploration Methods*: Geological Association of Canada, Mineral Deposits Division, Special Publication No. 5, p. 633-654.
- Paradis, S., Hannigan, P., and Dewing, K., 2007, Mississippi Valley-type lead-zinc deposits, in Goodfellow, W.D., ed., *Mineral Deposits of Canada: A Synthesis of Major Deposit-types, District Metallogeny, the Evolution of Geological Provinces, and Exploration Methods*: Geological Association of Canada, Mineral Deposits Division, Special Publication No. 5, p. 185-203.
- Peter, J.M., Kjarsgaard, I.M., and Goodfellow, W.D., 2003, Hydrothermal sedimentary rocks of the Heath Steele belt, Bathurst mining camp, New Brunswick: Part 1. Mineralogy and mineral chemistry, in Goodfellow, W.D., McCutcheon, S.R., and Peter J.M., eds., *Massive Sulfide*

Overview of Geophysical Signatures Associated with Canadian Ore Deposits

- Deposits of the Bathurst Mining Camp, New Brunswick, and Northern Maine: Economic Geology, Monograph, 11, p. 361-390.
- Reed, L.E., 1993, The application of geophysics to exploration for diamonds, in Dunne, K.P.E., and Grant, B., eds., Mid-Continent Diamonds: Geological Association of Canada – Mineralogical Association of Canada, Symposium Volume, p. 21-26.
- Reford, M.S., 1980, Magnetic method: Geophysics, v. 45, p. 1640-1658.
- Richardson, K.A., 1996, Part 3: Geophysical exploration and geographic information system (GIS) applications – Introduction, in Lecheminant, A.N., Richardson, D.G., DiLabio, R.N.W., and Richardson, K.A., eds., Searching for Diamonds in Canada: Geological Survey of Canada, Open File 3228, p. 225-228.
- Rowe, J.D., Smith, R.S., and Beattie, D., 1995, Geotem/aeromagnetic definition of hydrocarbon alteration plumes in Nevada: Geoterrex, CGG Canada brochure, reprinted from CGG World, v. 26, April 1995.
- Ruzicka, V., 1995, Unconformity-associated uranium, in Eckstrand, O.R., Sinclair, W.D., and Thorpe, R.I., eds., Geology of Canadian Mineral Deposit Types: Geological Survey of Canada, Geology of Canada, No. 8, p. 197-210 (also Geological Society of America, Geology of North America, v. P-1).
- Sangster, D.F., 1995, Mississippi Valley-type lead zinc, in Eckstrand, O.R., Sinclair, W.D., and Thorpe, R.I., eds., Geology of Canadian Mineral Deposit Types: Geological Survey of Canada, Geology of Canada, No. 8, p. 253-261 (also Geological Society of America, Geology of North America, v. P-1).
- Schiller, E.A., 1979, The history of uranium discoveries in northern Saskatchewan in the last decade, in Parslow, G.R., Uranium Exploration Techniques, 1978 November 16-17, Regina Symposium Proceedings: Saskatchewan Geological Society, Special Publication No. 4, p. 11-18.
- Scott, F., 1983, Midwest Lake uranium discovery, in Cameron, E.M., ed., Uranium Exploration in Athabasca Basin, Saskatchewan, Canada: Geological Survey of Canada, Paper 82-11, p. 41-50.
- Seigel, H.O., and Pitcher, D.H., 1978, Mapping Earth conductivities using a multifrequency airborne electromagnetic system: Geophysics, v. 43, p. 563-575.
- Seigel, H.O., Hill, H.L., and Baird, J.G., 1968, Discovery case history of the Pyramid orebodies Pine Point, Northwest Territories, Canada: Geophysics, v. 33, p. 645-656.
- Shives, R.B.K., and Holman, P.B., 1995, Digital Data for an Airborne Gamma-Ray Spectrometric, Magnetic, VLF-EM Survey, Paul Lake, Northwest Territories (parts of NTS 76D/9, 10): Geological Survey of Canada, Open File 3123.
- Shives, R.B.K., Ford, K.L., and Charbonneau, B.W., 1995, Applications of Gamma-Ray Spectrometric/Magnetic/VLF-EM Surveys – Workshop Manual: Geological Survey of Canada, Open File 3061, 82 p.
- Shives, R.B.K., Charbonneau, B.W., and Ford, K.L., 1997, The detection of potassic alteration by gamma-ray spectrometry - Recognition of alteration related to mineralization, in Gubins, A.G., ed., Proceedings of Exploration 97: Fourth Decennial International Conference on Mineral Exploration: Geophysics and Geochemistry at the Millennium, p. 741-752.
- Shives, R.B.K., Wasyluk, K., and Zaluski, G., 2000, Detection of K-enrichment (illite) chimneys using ground gamma ray spectrometry, McArthur River area, northern Saskatchewan, in Summary of Investigations 2000, Volume 2: Saskatchewan Geological Survey, Saskatchewan Energy Mines, Miscellaneous Report 2000-4.2, p. 160-169.
- Shives, R.B.K., Carson, J.M., Dumont, R., Ford, K.L., Holman, P.B., Diakow, L., 2004, Airborne multisensor geophysical survey, Toodoggone River Area, British Columbia (Parts of NTS 94D/15, E/2, 3, 5, 7, 10, 11): Geological Survey of Canada, Open File 4613, 1 CD-ROM.
- Sillitoe, R.H., 1979, Some thoughts on gold-rich porphyry copper deposits: Mineralium Deposita, v.14, p. 161-174.
- Sinclair, W.D., 2007, Porphyry deposits, in Goodfellow, W.D., ed., Mineral Deposits of Canada: A Synthesis of Major Deposit-Types, District Metallogeny, the Evolution of Geological Provinces, and Exploration Methods: Geological Association of Canada, Mineral Deposits Division, Special Publication No. 5, p. 223-243.
- Smith, R.J., 2002, Geophysics of iron oxide copper-gold deposits, in Porter, T.M., ed., Hydrothermal Iron Oxide Copper-Gold and Related Deposits: A Global Perspective, Volume 2: PGC Publishing, Adelaide, p. 357-367.
- Smith, R.S., Annan, A.P., Lemieux, J., and Pedersen, R.N., 1996, Application of a modified GEOTEM system to reconnaissance exploration for kimberlites in the Point Lake area, NWT, Canada: Geophysics, Society of Exploration Geophysists, v. 61, p. 82-92.
- St. Pierre, M., 1999, Geophysical properties of the BHP/Dia Met kimberlites, NWT Canada, in Lowe, C., Thomas, M.D., and Morris, W.A., eds., Geophysics in Mineral Exploration: Fundamentals and Case Histories: Geological Association of Canada, Short Course Notes, v. 14, p. 63-72.
- Telford, W.M., Geldart, L.P., and Sheriff, R.E., 1990, Applied Geophysics (Second Edition): Cambridge University Press, 770 p.
- Thomas, M.D., 1997, Gravity and Magnetic Prospecting for Massive Sulphide Deposits: A Short Course Sponsored under the Bathurst Mining Camp Extech II Initiative: Geological Survey of Canada, Open File 3514, 66 p.
- 2003, Gravity signatures of massive sulphide deposits, Bathurst Mining Camp, New Brunswick, Canada, in Goodfellow, W.D., McCutcheon, S.R., and Peter J.M., eds., Massive Sulfide Deposits of the Bathurst Mining Camp, New Brunswick, and Northern Maine: Economic Geology, Monograph, 11, p. 799-817.
- Thomas, M.D., and McHardy, S., in press, Magnetic insights into basement geology in the area of McArthur River uranium deposit, Athabasca Basin, Saskatchewan, in Jefferson, C.W., and Delaney, G., eds., EXTECH IV: Geology and Uranium EXploration TECHnology of the Proterozoic Athabasca Basin, Saskatchewan, and Alberta: Geological Survey of Canada, Bulletin 588 (Saskatchewan Geological Society, Special Publication 17; Geological Association of Canada, Mineral Deposits Division, Special Publication 4).
- Thomas, M.D., Walker, J.A., Keating, P., Shives, R., Kiss, F., and Goodfellow, W.D., 2000, Geophysical atlas of massive sulphide signatures, Bathurst Mining Camp, New Brunswick: Geological Survey of Canada, Open File 3887, New Brunswick Department of Natural Resources and Energy, Minerals and Energy Division, Open File 2000-4, 105 p.
- Tuach, J., Hewton, R.S., and Cavey, G., 1991, Exploration targets for volcanogenic, base-metal sulphide deposits on Pilley's Island, Newfoundland, in Ore Horizons, Volume 1: Newfoundland and Labrador Department of Mines and Energy, Geological Surveys Branch, p. 89-98.
- van Staal, C.R., 1994, Geology, Wildcat Brook, New Brunswick: Geological Survey of Canada, Map 1803A, scale 1:20 000.
- White, D.J., Hajnal, Z., Roberts, B., Gyorfi, I., Reilkoff, B., Bellefleur, G., Mueller, C., Woelz, S., Mwenifumbo, J., Takacs, E., Schmitt, D.R., Brisbin, D., Jefferson, C.W., Koch, R., Powell, B., and Annesley, I.R., in press, Seismic methods for uranium exploration: An overview of EXTECH IV seismic studies at the McArthur River mining camp, Athabasca Basin, Saskatchewan, in Jefferson, C.W., and Delaney, G., eds., EXTECH IV: Geology and Uranium EXploration TECHnology of the Proterozoic Athabasca Basin, Saskatchewan and Alberta: Geological Survey of Canada, Bulletin 588 (Saskatchewan Geological Society, Special Publication 17; Geological Association of Canada, Mineral Deposits Division, Special Publication 4).
- Wilford, J.R., Bierwirth, P.N., and Craig, M.A., 1997, Application of airborne gamma-ray spectrometry in soil/regolith mapping and applied geomorphology: AGSO Journal of Australian Geology and Geophysics, v. 17, p. 201-216.

Referenced Websites

- <http://www.bellgeo.com>
- <http://www.bhpbilliton.com>
- <http://www.fugroairborne.com>
- <http://www.eos.ubc.ca/ubcgif>
- <http://www.gov.nf.ca>
- <http://www.quantecgeoscience.com>
- <http://www.sgl.com>

Web Sites of Interest

Geophysics Courses

- <http://geo.polymtl.ca>, École Polytechnique de Montréal (Fr)
- <http://galitzin.mines.edu/INTROGP/index.jsp>, Colorado School of Mines (En)
- http://www.unites.uqam.ca/~sct/flux_de_chaleur/titre.html, UQAM (Fr)

<http://www-ig.unil.ch/cours/>, Université de Lausanne (En, Fr, Espagnol)
http://phineas.u-strasbg.fr/marquis/Enseignement/Public/Cours_Elmag/
EOST (Fr)
<http://www.geop.ubc.ca/ubcgif/tutorials/index.html>, UBC (En)
<http://courses.geo.ucalgary.ca/>, University of Calgary (En)
<http://www.usask.ca/geology/>, University of Saskatchewan (En)

Free Geophysics Books

<http://sepwww.stanford.edu/sep/prof/index.html>